Article

Not peer-reviewed version

Chemo-Diversity Landscape Using Physico-Biochemical, Elementals, and Metabolic Profiling in Different Stages and Accessions of *Madhuca longifolia* Flowers for Unveiling Their Processing Value and Utilization

Shalini Purwar , Ankit Verma , Ravi Prakash Jaiswal , Vigya Mishra , Vishal Chugh , Chandra Mohan Singh , Akbare Azam , Nitin Kumar , Priti Upadhyay , Tribhuvan Chaubey , Ashutosh Rai *

Posted Date: 26 February 2026

doi: 10.20944/preprints202602.1486.v1

Keywords: *Madhuca longifolia*; flower; ICPMS; gas chromatography; metabolities; minerals

 doi:10.20944/preprints202602.1486.v1

Article

Chemo-Diversity Landscape Using Physico-Biochemical, Elementals, and Metabolic Profiling in Different Stages and Accessions of *Madhuca longifolia* Flowers for Unveiling Their Processing Value and Utilization

Shalini Purwar [1,†], Ankit Verma [1,3,†], Ravi Prakash Jaiswal [2,†], Vigya Mishra [4], Vishal Chugh [2], Chandra Mohan Singh [5], Akbare Azam [2], Nitin Kumar [5], Priti Upadhyay [6], Tribhuvan Chaubey [7] and Ashutosh Rai [1,7,*]

[1] Department of Basic and Social Science, College of Forestry, BUAT, Banda- 210001, Uttar Pradesh, India
[2] Department of Basic and Social Science, College of Horticulture, BUAT, Banda- 210001, Uttar Pradesh, India
[3] Department of Chemistry, Government Girl's P.G. College, Ghazipur-233001, Uttar Pradesh, India
[4] Department of Post-Harvest Technology, College of Horticulture, BUAT, Banda- 210001, Uttar Pradesh, India
[5] Department of Genetics and Plant Breeding, College of Agriculture, BUAT, Banda- 210001, Uttar Pradesh, India
[6] Division of Vegetable Science, ICAR-Indian Agricultural Research Institute, New Delhi
[7] ICAR-Indian Institute of Vegetable Research, Varanasi-221305, Uttar Pradesh, India
* Correspondence: ashutoshraiiivr@gmail.com
† These authors contribute equally to this work.

Abstract

Variations in sweetness and bitterness among *Madhuca longifolia* flowers strongly influence their processing value and market acceptance, yet the chemo-diversity underlying these traits remains poorly characterized. This study aimed to unravel accession- and stage-specific differences by integrating physico-biochemical, elemental, and metabolic profiling across thirteen accessions (BM-1 to BM-13) from BUAT, Banda. Sensory and textural evaluations revealed wide diversity, with BM-5 displaying superior sweetness and aroma, whereas BM-6, BM-7, and BM-10 were differentiated by firmness, elasticity, and gumminess. Biochemical analyses across flower development showed BM-5 consistently maintained higher sugars and β-carotene, while BM-1 exhibited marked reductions in sugars and total phenolics content; antioxidant activity increased with maturity, with BM-5 remaining the most stable. ICP-MS elemental analysis confirmed BM-5 as mineral-rich compared with lower-performing accessions. GC–MS metabolomic profiling of contrasting accessions (BM-1 and BM-5) across stages identified 376 volatile and semi-volatile metabolites, and multivariate analyses (PCA, VIP, volcano plots, pathway enrichment) revealed distinct stage- and accession-dependent patterns. Mature BM-5 was enriched in fermentation- and aroma-related metabolites such as melibiose, furfural, 5-HMF, and furaneol, whereas BM-1 accumulated defense-linked compounds including catechol, benzyl nitrile, and maltol. Overall, the integrated chemo-diversity landscape identifies BM-5 as a superior accession with high processing potential and value-addition prospects.

Keywords: *Madhuca longifolia*; flower; ICPMS; gas chromatography; metabolities; minerals

1. Introduction

Madhuca. longifolia J.F. Macbr. (Mahua) plays a significant role in the socioeconomic development and nutritional security of ethnic tribes across several Southeast Asian countries, including India,

 doi:10.20944/preprints202602.1486.v1

Indonesia, Myanmar, Sri Lanka, and Nepal [1]. *M. longifolia* flowers are edible and rich in fermentable sugars and phytochemicals, making them an excellent food supplement. Traditionally, they are consumed in various forms, including raw, roasted, boiled, and processed [2]. According to the Forest Governance Learning Group India (2018), out of 490,000 tonnes of *M. longifolia* flowers harvested annually, only 85,000 tonnes are utilized, and approximately 17.55% of India's workforce is engaged in *M. longifolia* flower collection [3]. Dried *M. longifolia* flowers represent a low-cost renewable biomass that could serve as a carbon source, although their cost-effectiveness depends on carbohydrate content and recovery efficiency relative to purified glucose. [4].

Fermentation plays a crucial role in the food and beverage industries by enhancing sensory appeal, nutritional quality, and shelf life. Consumers increasingly prefer fermented juices due to their improved flavor and enriched vitamin and mineral content [1]. Technological advancements have facilitated the development of value-added products from underutilized biomaterials, with studies reporting effective pre- and post-fermentation strategies that enhance bioactive compounds and functional attributes [1,5,6]. Several investigations have examined the composition and quality of *M. longifolia* flowers, including their antioxidant activity, mineral content, and chemical constituents [4], their application in producing low-alcoholic beverages [7], fumaric acid extraction using *Rhizopusoryzae* [4], and the identification of *Meyerozymacaribbica* M72 for saccharification and ethanol production [8].

M. longifolia flowers hold significant cultural and economic importance across tribal and rural India. However, considerable variation exists among different *M. longifolia* accessions in terms of sweetness, bitterness, and the metabolite profiles that shape their aroma, flavor, fermentability, and nutritional properties. These sensory and biochemical differences directly influence both market value and processing suitability, yet they cannot be adequately assessed through conventional sensory tests or basic chemical analyses alone. Therefore, advanced analytical approaches are essential for objective characterization. Gas chromatography (GC/GC–MS) is particularly valuable, as it provides precise qualitative and quantitative profiling of key metabolites, enabling reliable comparison between varieties and supporting quality assurance for diverse industrial applications.

In the present study, we integrate sensory and instrumental texture profiling with biochemical analyses to explore the primary metabolites, mineral composition, and volatile profiles of *M.longifolia* flowers across developmental stages in contrasting accessions. The volatile metabolite profiling was performed using GC–MS, while mineral quantification was achieved through ICP-MS, resulting in a comprehensive dataset for examining developmental dynamics. Variable Importance in Projection (VIP) analysis was used to identify the most influential GC–MS features contributing to sample variation, enabling the selection of significant biomarkers and enhancing model interpretability in complex chromatographic datasets. To further understand metabolic changes, KEGG pathway mapping was conducted to reveal regulatory networks associated with flower maturation. Through the integration of statistical modeling and metabolic pathway analysis, this study provides a holistic understanding of how primary metabolites, minerals, and volatile compounds are dynamically regulated during floral development, highlighting accession-specific metabolic signatures relevant for conservation, valorization, and potential industrial applications of *M. longifolia*.

2. Results

Thirteen accessions (BM-1 to BM-13) of*M.longifolia* collected from the BUAT orchard were evaluated for textural and sensory attributes. Based on these assessments, selected accessions were further subjected to biochemical analyses at two developmental stages, namely immature and mature flower stages. Elemental profiling using ICP-MS was conducted at the mature flower stage. In addition, selected contrasting accessions were subjected for GC–MS analysis at both developmental stages to elucidate the metabolic basis of sensory and aroma attributes.

 doi:10.20944/preprints202602.1486.v1

2.1. Texture and Sensory Analysis of Flowers from Different Accessions of M. longifolia

Texture analysis of *M. longifolia*flower accessions (BM-1 to BM-13) collected from the BUAT, Banda campus was performed using a TA.XT Express Connect Texture Analyser. Parameters such as skin strength, elasticity, hardness, springiness, and gumminess were assessed. BM-6 exhibited the highest skin strength (139.14 ± 37.65) and hardness (136.59 ± 0.22), indicating a firm texture. BM-7 showed maximum elasticity (5.95 ± 0.98 mm), while BM-4 demonstrated the highest springiness (103.91 ± 0.66). BM-10 recorded the highest gumminess (50.11 ± 0.98)Supplementary table S1 and **Figure 1a**. Sensory evaluation on a 10-point hedonic scale identified BM-5 as the most preferred accession due to its highest sweetness (8.18 ± 0.44) and aroma (8.1 ± 0.39) scores. BM-1,moderate in sweetness, exhibited superior texture firmness and stability, indicating better shelf-life potential **Figure 1b**. Based on overall sensory and texture performance, BM1, BM-4, BM-5, BM-6 and BM-10were selected for further biochemical analysis.

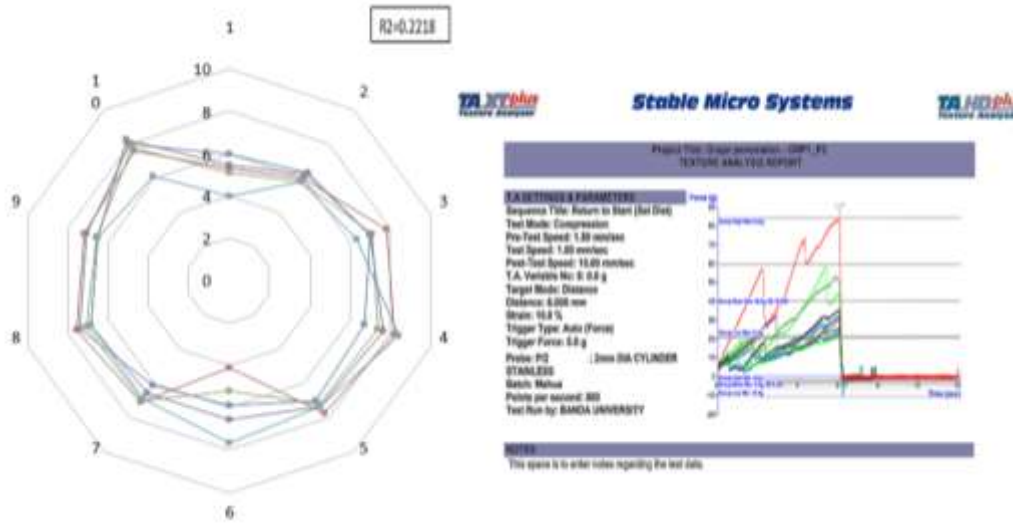

Figure 1. a) The sensory analysis using a 10-point hedonic scale revealed that different accessions(BM1-BM13) of *M. longifolia* flowers significantly impacted attributes like taste, aroma, texture, and overall consumer acceptance, with some accessions excelling in multiple sensory properties.**b)** Texture data to evaluate the quality of *M. longifolia* Flower in different accession.

2.2. The Biochemical Analysis of Primary Metabolites During Developmental Stages of Flowering in Selected Accession of M. longifolia

Biochemical analysis of five selected *M. longifolia* accessions (BM-1, BM-4, BM-5, BM-6, and BM-10) during flower developmental stages (immature to mature) revealed significant variation in metabolite profiles. Total sugar content increased with maturity, with the highest levels in BM-5, whereas BM-1 showed a sharp decline. Reducing sugar high in immature but non-reducing sugars high at mature flowering stage; BM-10 exhibited the highest reducing sugar in immature flowers, while BM-6 had the highest in mature flowers. Vitamin C, β-carotene, the total phenolics content (TPC), crude fiber, and protein decreased with flower maturation, whereas lycopene content and antioxidant activity (DPPH) increased, indicating enhanced oxidative defense in mature flowers. Betanin showed variable trends, increasing in BM-5 but slightly decreasing in BM-10 (Figure 2a–kOverall, BM-5 exhibited superior biochemical stability, higher sugar retention, and enhanced antioxidant and sensory attributes, indicating its potential as a high-quality accession. In contrast, BM-1 showed comparatively lower biochemical stability and reduced quality-related parameters. Based on these contrasting biochemical profiles, BM-1 and BM-5 were selected for further elemental profiling and gas chromatography analysis to elucidate compositional differences associated with quality traits.

 doi:10.20944/preprints202602.1486.v1

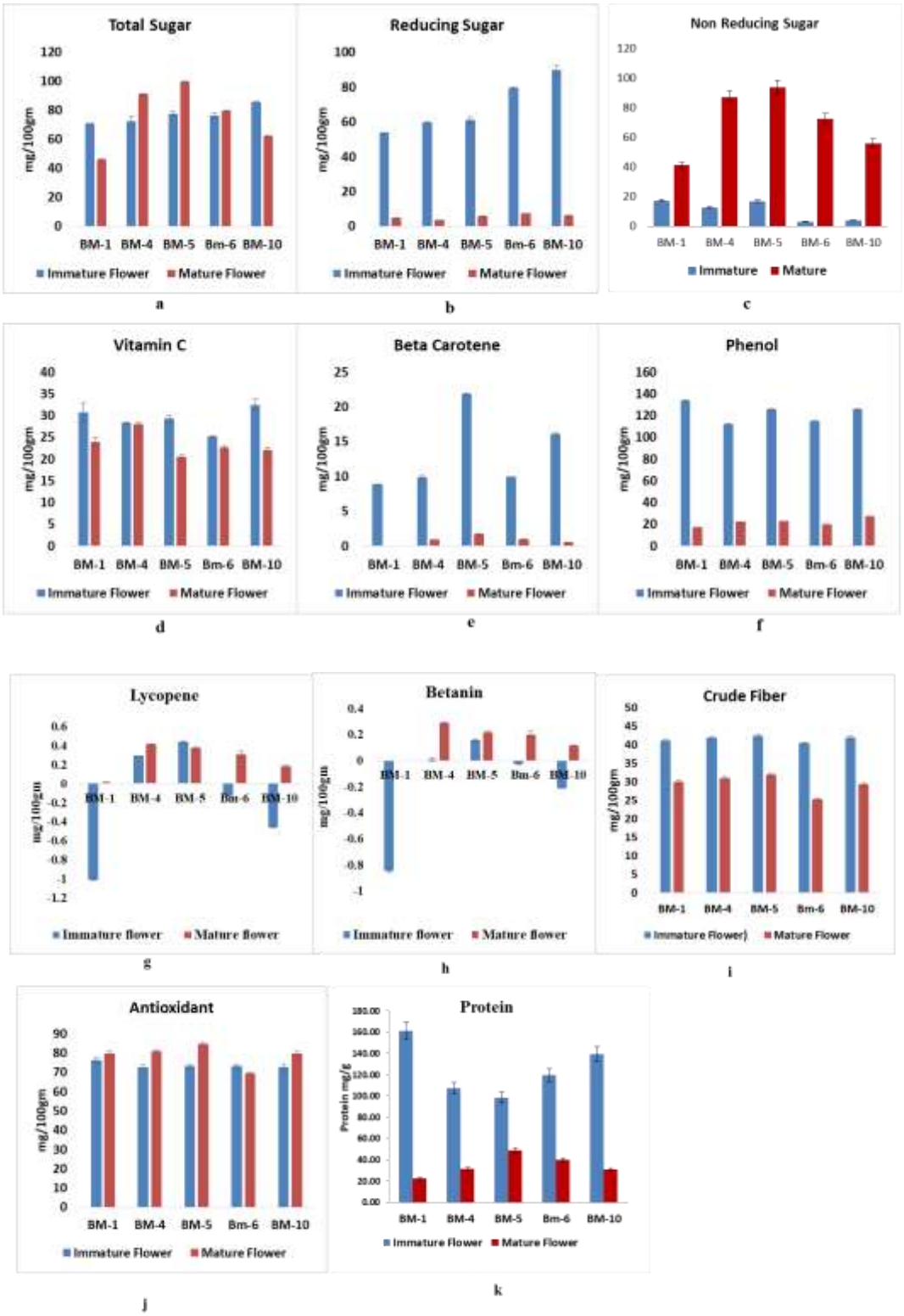

Figure 2. The biochemical analysis of primary metabolites in different accessions *of M.longifolia* flowers during developmental stages (from immature flowers to mature flowers)reveals significant variations in metabolite levels, reflecting dynamic biochemical changes during flower maturation. a) Total Sugar, b) Reducing c) non-reducing sugar d) Vitamin C, e) Beta-carotene, f) Phenol g) lycopene h) Betanin, i) crude fiber j) Antioxidant properties k) Protein.

 doi:10.20944/preprints202602.1486.v1

2.3. Elemental Composition of M. longifolia Flower in Contrasting Accessions by ICP–MS

Elemental profiling of two contrasting*M. longifolia* accessions (BM1 &BM5),mature flowersusing inductively coupled plasma mass spectrometry (ICP–MS) revealed distinct differences in mineral composition. Among the elements detected, magnesium and calcium were present in higher concentrations than other minerals. Magnesium levels were similar in both accessions, while calcium concentration was higher in BM-5. Iron concentrations differed slightly between the BM1 and BM5 accessions, with the BM-5 accession having higher iron levels (83.17ppm) than the BM1 accession (79.74ppm). Other trace elements, such as sodium, phosphorus, manganese, iron, cobalt, copper, and zinc, were found in comparatively lower amounts, but their relative distribution varied between accessions (Figure 3). These results demonstrate mineral diversity within *M. longifolia* accessions, suggesting that different accessions could serve as potential sources of specific micronutrients. Such variability detected by ICP–MS analysis provides valuable information for nutritional evaluation.

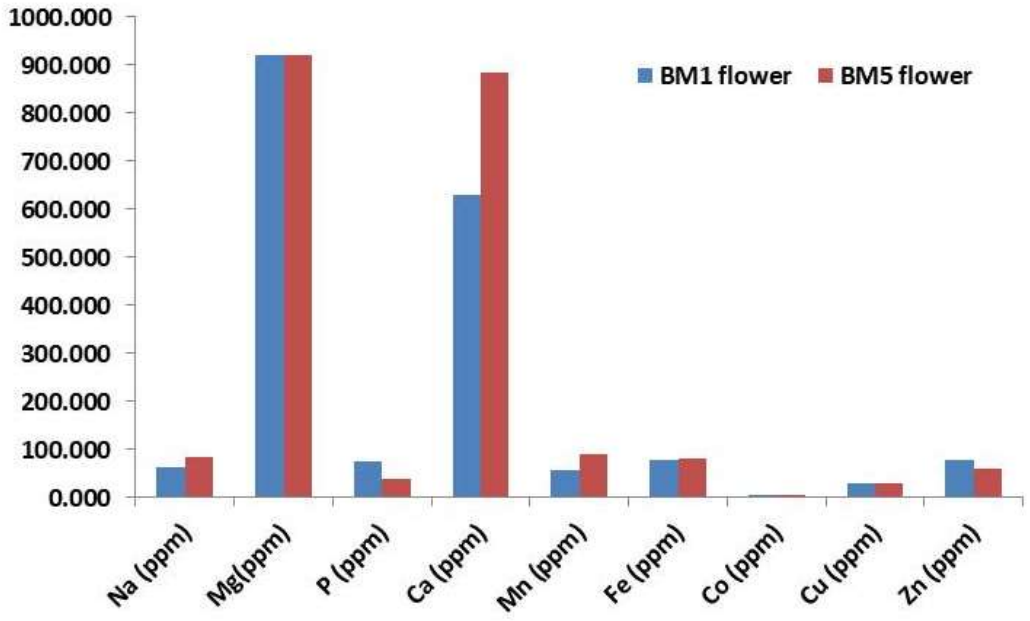

Figure 3. ICP–MS–based ionomic profiling of *M. longifolia*mature flowers in c**ontrasting**accessions BM-1 and BM-5.

2.4. GC–MS-Based Metabolite Profiling and Pathway Enrichment Analysis During Developmental Stages of Flowering in Contrasting M. longifoliaaccessions

GC–MS chromatograms of volatile and semi-volatile compounds in two contrasting *M. longifolia* accessions (BM-1 and BM-5) across immature (IMF) and mature (MF) floral stages identified 60, 65, 94, and 84 metabolites in BM-1(IMF), BM-5(IMF), BM-1(MF), and BM-5(MF), respectively(Figure 4a,b,c,d**)** and (Supplementary Tables S2a,b and S3a,b). Venn analysis showed BM-5(MF) had the highest number of unique metabolites [48], followed by BM-5(IMF) [43], while BM-1(IMF) and BM-1(MF) contained only 25 and 27 unique compounds, reflecting a more limited biochemical spectrum. Twelve metabolites were common to all four groups, with additional partial overlaps indicating stage- and accession-specific divergence (Figure 4e). PCA explained 89.6% of the total variance (PC1: 63.09%, PC2: 14.54%, PC3: 12.08%), and the 3D plot revealed clear clustering by accession and developmental stage. BM-5(MF) separated strongly along PC1, while BM-1(IMF) grouped distinctly along PC2, confirming contrasting metabolic trajectories between the two accessions during flower development (Figure 4f).

 doi:10.20944/preprints202602.1486.v1

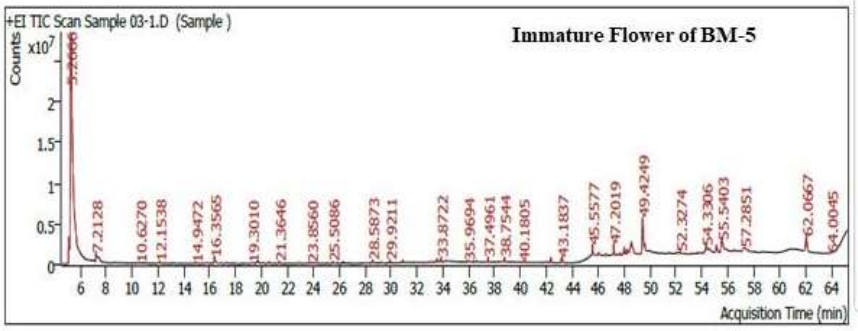

(a)

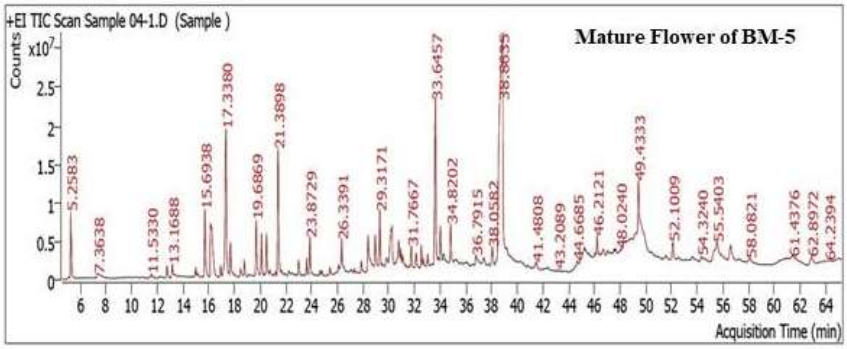

(b).

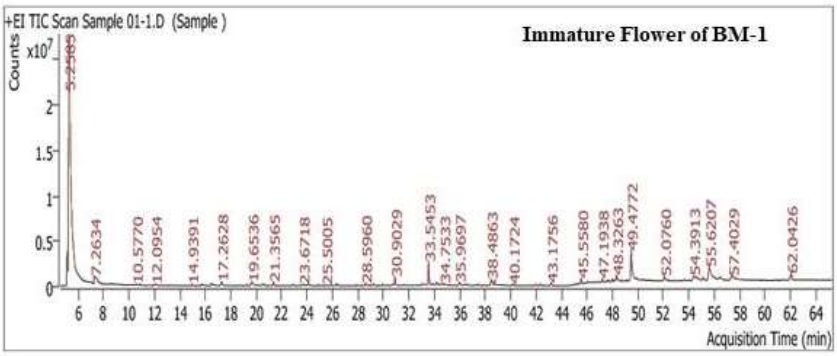

(c).

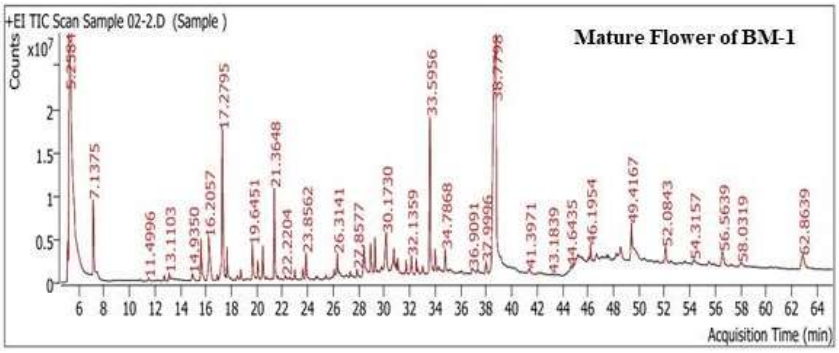

(d).

 doi:10.20944/preprints202602.1486.v1

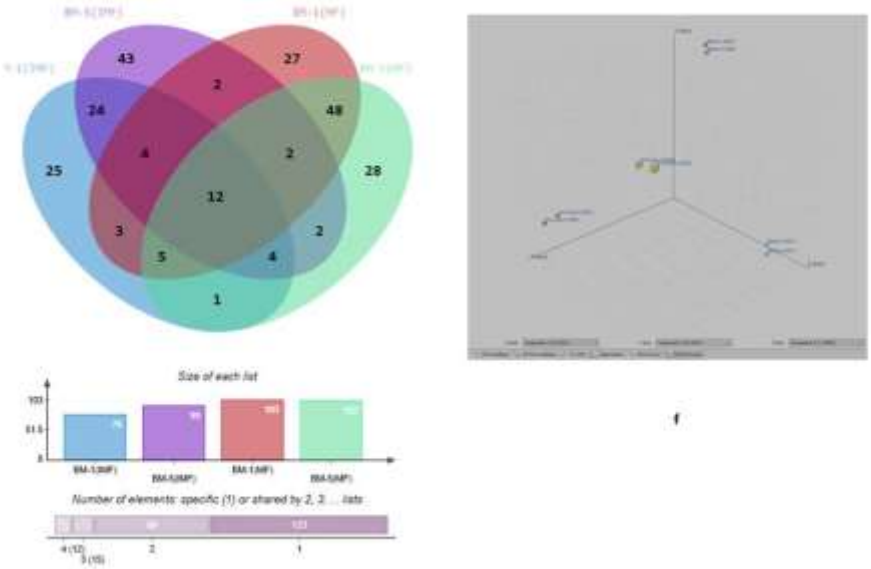

Figure 4. GS-Chromatogram highlighting accession-specific differences in metabolite composition of *M. longifolia* flowers **a)** at Immature Flower stages of BM-5 **b)** Flower stages of BM-5. **c)** Immature Flower stages of BM-1 **d)** Mature Flower stages of BM-1 **e)**Comparison of metabolite distribution between developmental stages of *M. longifolia* flowers, highlighting stage-specific and common compounds by Venna diagramme. **f)** Principal Component Analysis (PCA) score plot showing metabolite clustering in *M. longifolia* flowers during developmental stages and accessions (BM-1 and BM-5).

Integrated KEGG pathway enrichment revealed clear metabolic variation among *M. longifolia* accessions and developmental stages. All four groups—BM-1(IMF), BM-5(IMF), BM-1(MF), and BM-5(MF)—shared enrichment in pathways. BM-1(MF) showed the highest pathway diversity, in ABC transporters, amino acid biosynthesis, and multiple degradation pathways, indicating a highly active metabolic state in mature flowers. BM-5 (MF) also shows pathway enrichment, particularly in microbial metabolism and secondary metabolite biosynthesis, although the total number of enriched pathways is slightly lower than in BM-1 (MF). In contrast, the immature flower groups (BM-1 IMF and BM-5 IMF) display relatively fewer enriched pathways, though they still include key processes such as furfural degradation and biosynthesis of plant secondary metabolites (Figure 5a).

Venn analysis showed 26 pathways common to all groups, representing core metabolism. BM-1(IMF) was metabolically most distinct with 38 unique pathways, followed by BM-5(IMF) (18 unique). In contrast, mature flowers displayed greater similarity, with only 3 and 2 unique pathways in BM-1(MF) and BM-5(MF), respectively, indicating metabolic convergence with maturation (Figure 5a &b). Overall, developmental stage exerted a stronger influence than accession, with BM-1 immature flowers being the most distinct and BM-1 mature flowers showing the highest enrichment in pathways related to flavor, aroma, and physiological adaptation. These results underscore *M. longifolia* flowers as valuable sources of bioactive and aromatic compounds.

 doi:10.20944/preprints202602.1486.v1

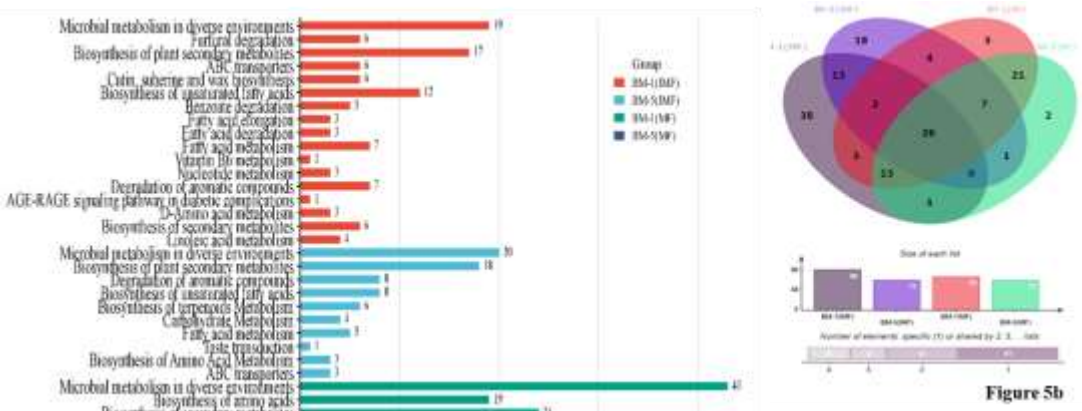

Figure 5a

Figure 5b

Figure 5. a) KEGG pathway analysis of GC–MS–identified metabolites from *M. longifolia* flowers (BM-1 and BM-5), showing enriched biochemical pathways and metabolite counts. **b)**Venna diagramme Comparison of pathway analysis between developmental stages of *M. longifolia* flowers, highlighting stage-specific pathways by Venna diagramme.

2.5. Hierarchical Clustering, and Variable Importance in Projection (VIP) Score, Analysis in and Volcano Plot-Based Differential Metabolite Profiling Developmental Stages of Flowering in Contrasting Accession of M. longifolia

The clustered heatmapdendrogram offers a global view of the volatile and semi-volatile metabolite profiles during*M. longifolia*developmental flower groups: BM1-IMF, BM5-IMF, BM1-MF, and BM5-MF. The dendrogram reveals that the primary separation among samples is based on developmental stage rather than accession. Mature flower samples (BM1-MF and BM5-MF) form one cluster, while immature samples (BM1-IMF and BM5-IMF) form another, indicating greater similarity in metabolite composition within each developmental phase. (Figure 6a).

The VIP score–based heat map revealed clear differences in aroma- and taste-related metabolites among the accessions. Although BM1 exhibited several high-VIP compounds, these were mainly associated with green and immature, including short-chain alcohols and aldehydes, which contribute to aroma intensity but not necessarily to desirable taste. In contrast, BM5 showed a greater contribution of furan, furanone, and pyran derivatives, which are known to impart sweet, caramel-like, and pleasant roasted aromas, indicating superior flavor quality. The BM5 samples, particularly at the immature stage, displayed fewer aroma-active compounds with lower VIP contributions, resulting in a comparatively mild sensory profile. Overall, the results demonstrate that BM5 possesses the most favorable aroma and taste characteristics, while BM1, despite higher discriminating metabolite abundance, exhibits inferior sensory quality due to the predominance of immature aroma compounds (Figure 6b and Supplementary Table S4). Overall, the combined clustering and VIP analyses demonstrate that developmental stage is the primary driver of metabolic differentiation in *M. longifolia* flowers.

 doi:10.20944/preprints202602.1486.v1

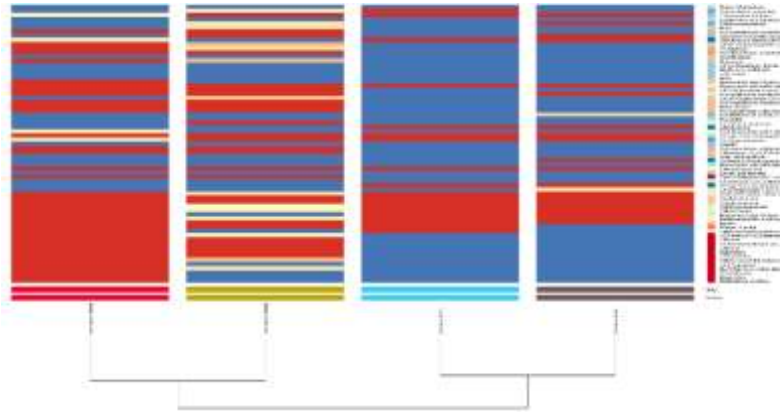

a

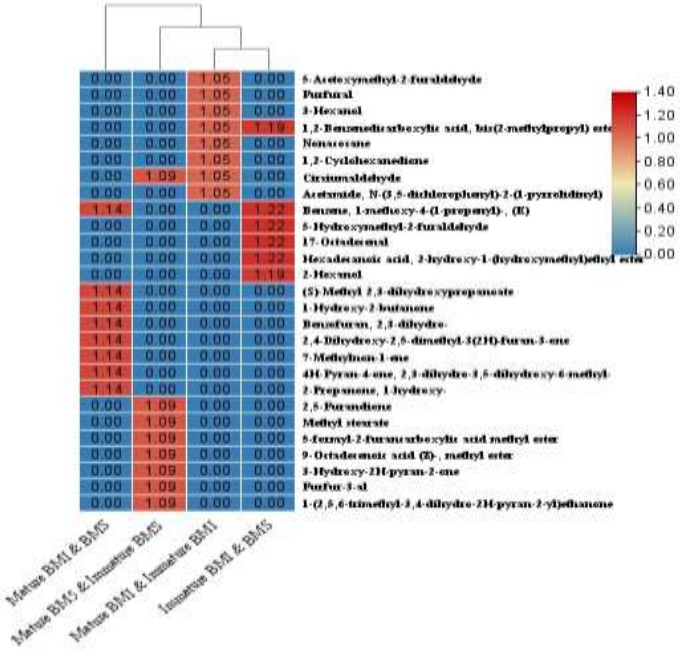

b

Figure 6. a) Fingerprinting analysis of volatile metabolites in *M. longifolia*flowers during developmental transitions (immature to mature flower stage), generated through GC–MS profiling. Distinct colors represent stage-specific accumulation and diversity of compounds.b) VIP score plot derived from PLS-DA analysis highlighting key metabolites of taste and Aroma contributing to stage- and accession-specific variation in *M. longifolia* flowers.

Metabolomic profiling of *M. longifolia* flowers using volcano plot analysis revealed significant stage- and accession-specific metabolic alterations between BM-1 and BM-5. In immature flowers, BM-5 showed strong upregulation of key metabolites such as Hexadecanoic acid, 2-Hydroxy-1-(hydroxymethyl) ethyl ester (23.1-fold), 17-Octadecenal (19.4-fold), and 5-Hydroxymethyl-2-furaldehyde (5-HMF) (21.8-fold). Nitrogenous and phenolic volatiles, including Benzyl nitrile and 4-Hydroxybenzaldehyde, were also significantly elevated in BM-5. In mature flowers, BM-5 exhibited marked upregulation of metabolites such as, Hexamethyl-, 5-HMF, and 3H-Pyrazol-3-one derivative, while compounds like 4H-Pyran-4-one, 3, 5-Dihydroxy-2-methyl- and Hexadecamethyl- were downregulated, implying a shift from sugar-derived intermediates to secondary metabolites. Transition from immature to mature stages in BM-5 was characterized by enhanced accumulation of methyl esters (e.g., Methyl stearate, Linoleic acid methyl ester), reinforcing floral aroma and cuticle development (Figure 7a,b and c and Supplementary Table S5).

 doi:10.20944/preprints202602.1486.v1

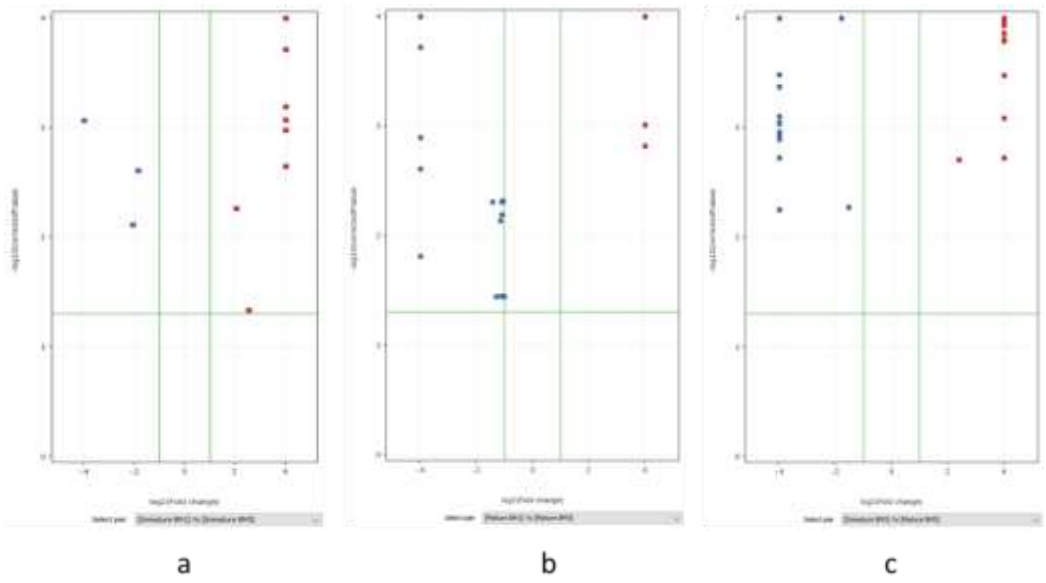

Figure 7. Volcano plot showing differential metabolite accumulation between Immature and mature *M. longifolia* accessions BM-1 and BM-5. a) Immature BM1 vs. Immature stages of BM-5; (b) Mature BM1 vs. Mature flower stages of BM-5; (c) Immature BM-5 vs. Mature flower BM-5. The x-axis represents $\log_2$(fold change), and the y-axis indicates $-\log_{10}$(corrected p-value). Each point corresponds to a metabolite detected by GC–MS. Red dots represent significantly upregulated metabolites in BM-5, blue dots indicate those enriched in BM-1, while grey dots denote non-significant metabolites. Vertical and horizontal green lines mark the thresholds for fold change (±2) and significance ($p < 0.05$).

2.6. Regulation of Key Metabolite During Developmental Stages of Flowering in Contrasting Accession of M. longifolia

GC–MS peak areas were used for relative metabolite quantification, and normalized values were applied to assess metabolic variation across floral developmental stages and contrasting *M.longifolia* accessions. GC–MS profiling revealed dynamic changes in sugars, fatty acid derivatives, furan compounds, and pyranone derivatives, indicating their roles in floral development, aroma formation, and accession-specific metabolic differentiation. These stage-dependent variations suggest coordinated biochemical regulation during flower maturation.

2.6.1. Metabolic Regulation of Sugars and Its Derivatives During Developmental Stages of Flowering in Contrasting Accession of *M. longifolia*

Sugar metabolism showed clear developmental and accession differences. β-D-Glucopyranose, 1,6-anhydro- also known as levoglucosan washigher in BM-5 immature flowers (4.65) than BM-1 (0.70) but declined at maturity. D-Allose was detected only in BM-1 mature flowers (0.88), while Melibioseaccumulated in BM-5 mature flowers (2.66), indicating accession-specific roles in maturation. 1,3,4,5-Tetrahydroxycyclohexane carboxylic acid (Quinic acid) was present across all stages, with higher levels (~3.0%) in immature flowers of both accessions and lower (~1.0–1.5%) at maturity**.** Flavone 4′-OH,5-OH,7-di-O-glucosideoccurred only in immature flowers, being higher in BM-1 (1.76). Beta-Amyrin was absent in immature stages and BM-1 mature flowers but appeared specifically in BM-5 mature flowers (~0.5–1.0%). (Figure 8a).

 doi:10.20944/preprints202602.1486.v1

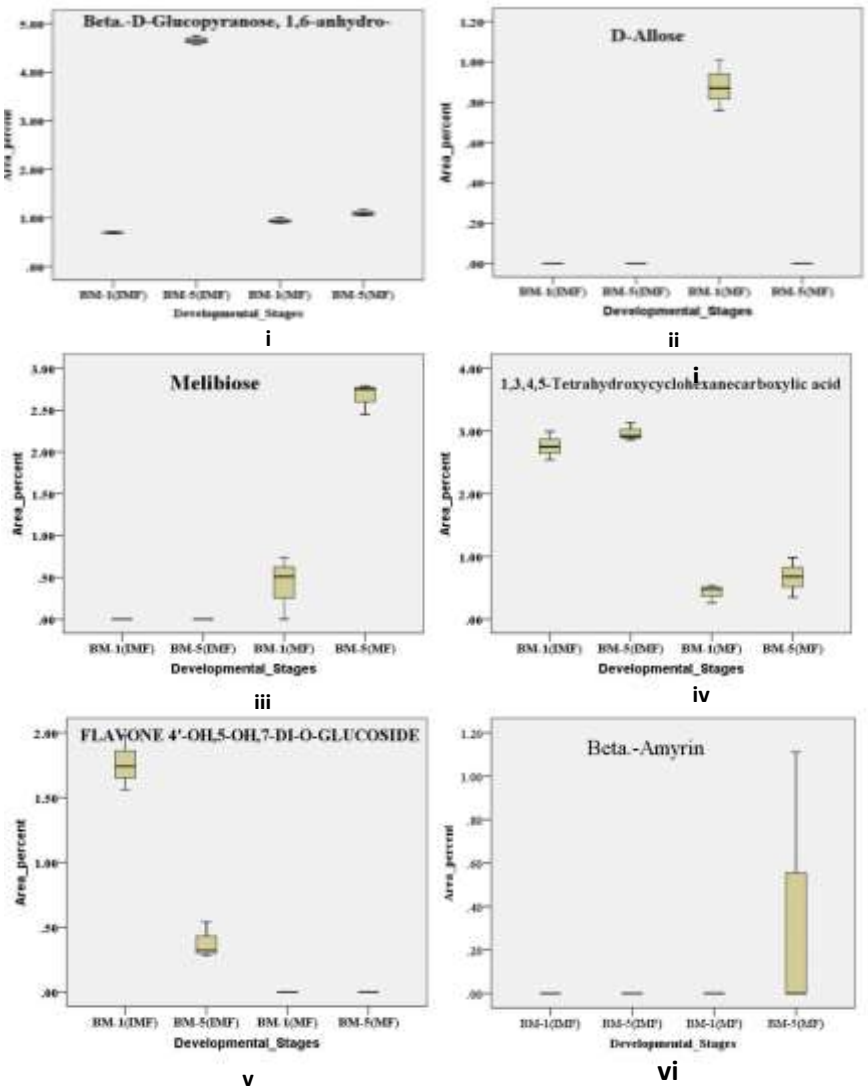

(a)

 doi:10.20944/preprints202602.1486.v1

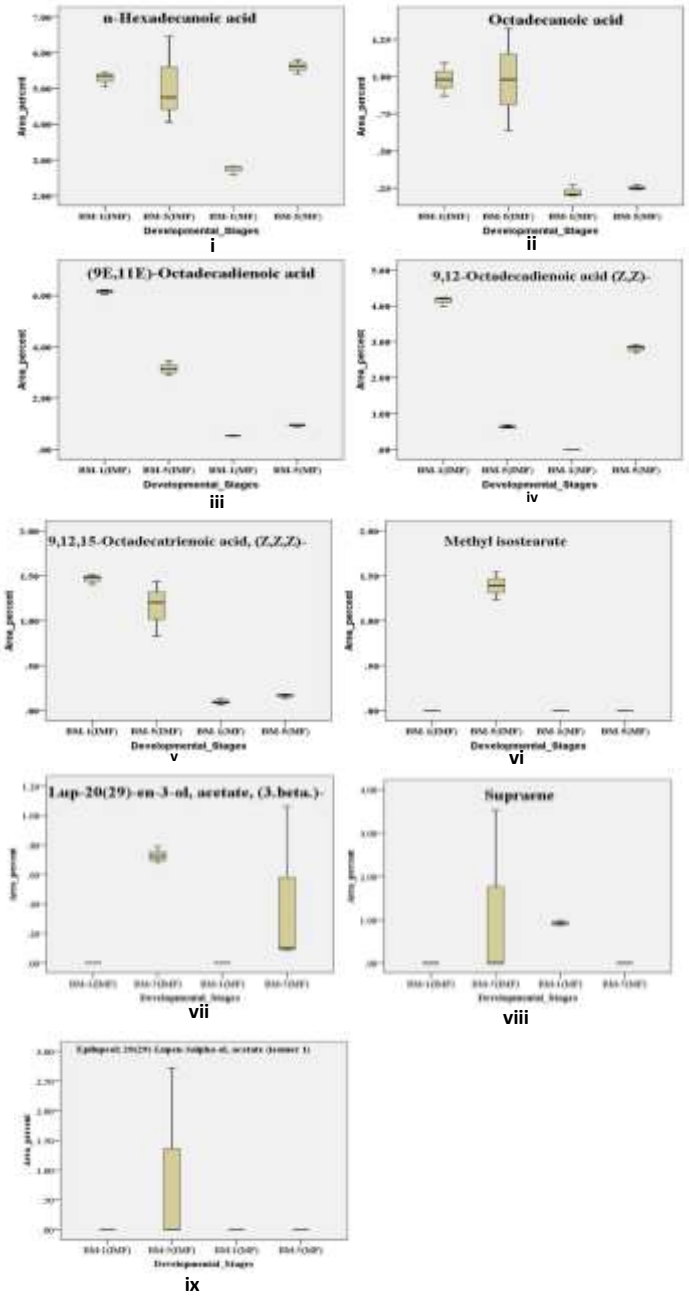

(**b**)

 doi:10.20944/preprints202602.1486.v1

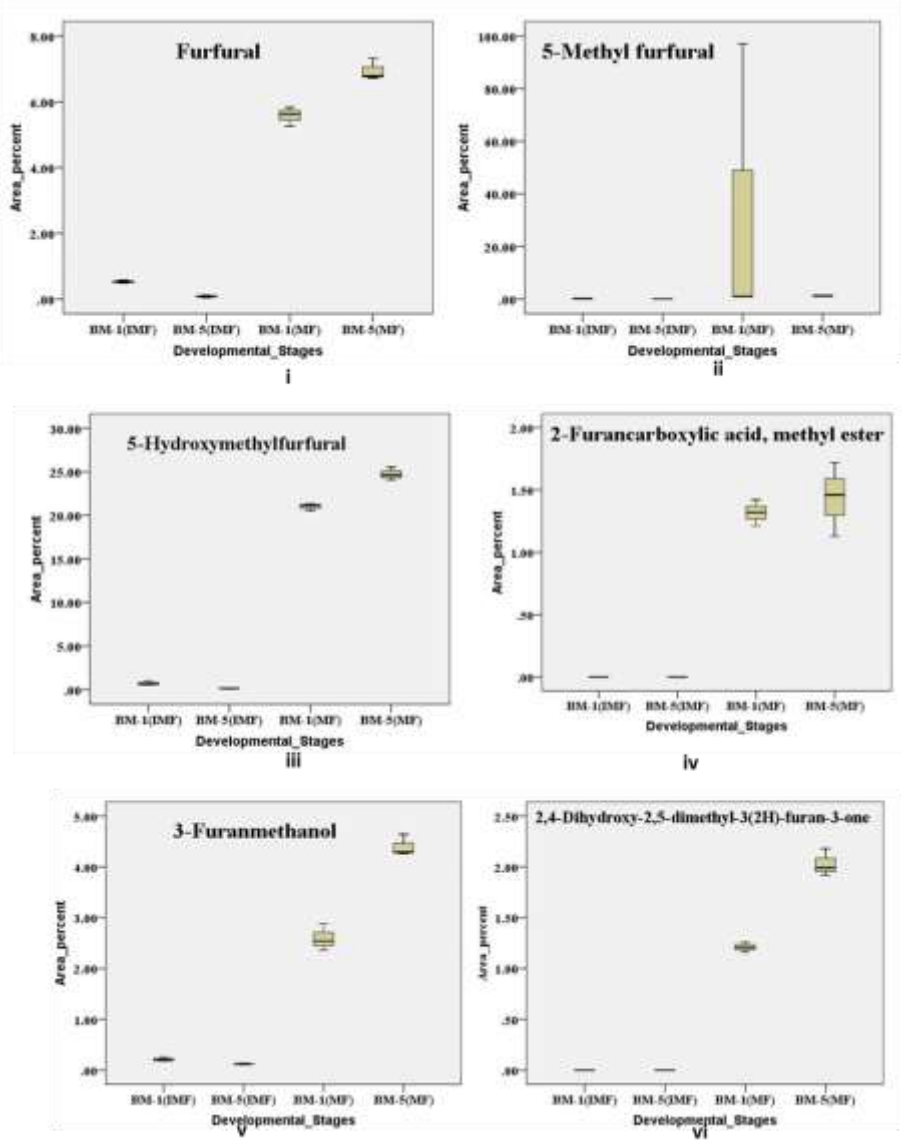

(c)

 doi:10.20944/preprints202602.1486.v1

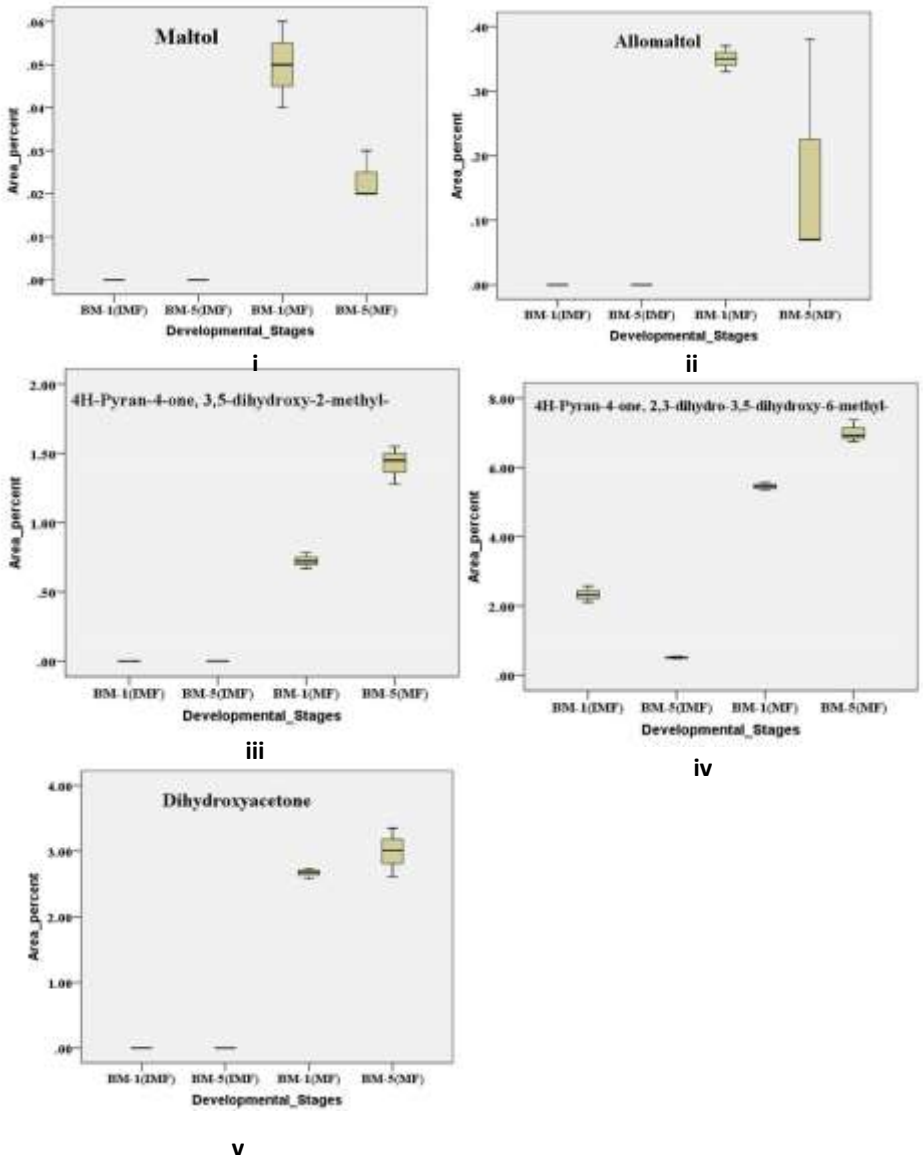

(**d**)

Figure 8. a: Boxplot representation of key Sugars and its Derivatives metabolites identified in *M. longifolia* flowers during developmental stages in contrasting accessions (BM-1 and BM-5). The plots show relative abundance of (i) Beta-D-Glucopyranose, 1,6-anhydro-, (ii) D-Allose, (iii) Melibiose, (iv) 1,3,4,5-Tetrahydroxycyclohexane carboxylic acid, (v) Flavone-4′-O-β-D-glucoside, and (vi) Beta-Amyrin. Data illustrate stage-specific and accession-specific metabolite accumulation patterns. **b.** Boxplot representation of key fatty acid–derived and terpenoid metabolites identified in *M. longifolia* flowers during developmental stages in two contrasting accessions (BM-1 and BM-5). The plots show the presence of (i) Hexadecanoic acid, (ii) Octadecanoic acid, (iii) (9E,11E)-Octadecadienoic acid, (iv) 9,12-Octadecadienoic acid (v) 9,12,15-Octadecatrienoic acid (vi) Methyl isostearate, (vii) Lup-20(29)-en-3β-ol acetate, (viii) Suprane, and (ix) Epilupeol [20(29)-lupen-3α-ol] acetate. The boxplots illustrate stage-specific and accession-specific patterns of metabolite accumulation during flower development. **c.** Boxplot representation of key furan-derived metabolites identified in *M. longifolia* flowers during developmental stages in two contrasting accessions (BM-1 and BM-5). The plots depict the presence of (i) furfural, (ii) 5-methylfurfural, (iii) 5-hydroxymethylfurfural, (iv) 2-furan carboxylic acid, (v) 3-furanmethanol, and (vi) 2,4-dihydroxy-2,5-dimethyl-3(2H)-furan-3-one. The boxplots illustrate stage-specific and accession-specific variations in metabolite accumulation during flower development. **d.** Boxplot representation of key Pyranoneand its -derived metabolites identified in *M. longifolia* flowers during developmental stages in two contrasting accessions (BM-1 and BM-5). The panels represent the relative abundance of (i) Maltol, (ii) Allomaltol, (iii) 4H-Pyran-4-one, 3,5-dihydroxy-2-methyl-, (iv) 4H-Pyran-4-one, 2,3-dihydro-3,5-dihydroxy-6-

 doi:10.20944/preprints202602.1486.v1

methyl-, and (v) dihydroxyacetone. The boxplots illustrate stage-specific and accession-specific variations in metabolite accumulation during flower development.

2.6.2. Metabolic Regulation of Fatty Acids Derivative Contributes During Developmental Stages of Flowering in Contrasting Accession of M. longifolia

Lipid profiling showed stage- and accession-specific shifts. n-Hexadecanoic acid (palmitic acid) was consistently abundant, especially in BM-1(IMF: 5.28) and BM-5(MF: 5.61), implying structural roles. Octadecadienoic acid higher in mature Flower stage of BM1while absent at BM-5 mature stage. (9E,11E)-Octadecadienoic acid peaked in BM-1(IMF: 6.15), while 9,12-Octadecadienoic acid (linoleic acid) was found in BM-1(IMF: 4.14) and BM-5(MF: 2.81). 9, 12, 15 Octodecatrienoic acid at immature stage, Methyl isostearate was unique to BM-5(IMF: 1.39), suggesting active fatty acid methylation. among terpenoid-derived compounds, Lup-20(29)-en-3-ol, acetate (3β-) also known asLupeol acetate,Supraene, and Epilupeolwere absent at the BM-1 immature stage but present in BM-5 immature flowers, with Lup-20(29)-en-3-ol, acetate (~2.0%) and Epilupeol (~1.5%) showing the abundance, while Supraene reached ~1.5%. At maturity, their levels declined sharply, with only low amounts of Lup-20(29)-en-3-ol, acetate (~1.0%) and Supraene (~1.0% in BM-1 mature) detected, whereas Epilupeol was undetectable, indicating their preferential role during immature flower development. (**Figure 8b)**

2.6.3. Metabolic regulation of Furan and Furan Derivative Contributes During Developmental Stages of Flowering in Contrasting Accession of *M. longifolia*

Furan-related volatiles increased during maturation. Furfural and 5-Hydroxymethylfurfural (HMF) were highly elevated in BM-5(MF: 6.94 and 24.74), respectively, indicating sugar dehydration and oxidative metabolism. 5-Methyl furfural was highest in BM-1(MF: 33.02), while 2 Furancorboxylic acid, Methyl ester, 3-Furanmethanol and 2,4 Dihydroxy-2-5 dimethyl-3(2H)-Furan-3-one (also known as Furaneol) derivatives appeared predominantly in mature BM-5 flowers, suggesting a link to floral scent and late-stage stress responses (Figure 8c).

2.6.4. Metabolic Regulation of Pyranone and Its Derivative Contributes During Developmental Stages of Flowering in Contrasting Accession of *M. longifolia*

During the developmental progress of *M. longifolia* flowers, pyranone derivatives showed stage-specific patterns. Maltol and Allomaltol were absent at the immature bud stage (BM-1) but accumulated significantly at maturity, with higher abundance in BM-1 mature flowers compared to BM-5**.** 4H-Pyran-4-one, 3,5-dihydroxy-2-methyl, a hydroxylated derivative of Maltol, was undetectable in early buds but increased steadily, reaching maximum levels at BM-5 mature flowers. In contrast, 4H-Pyran-4-one, 2,3-dihydro-3,5-dihydroxy-6-methyl (hydroxydihydromaltol, was higher in BM-1 immature buds, decreased at BM-5, and rose again at maturity**.** Dihydroxyacetone (DHA)**,** absent in early buds, appeared at the mature stage of BM-1 and remained significant in BM-5, reflecting active carbohydrate metabolism (Figure 8d).

3. Discussion

3.1. Texture and Sensory Analysis of Flowers Collected from Different Accessions of M. longifolia

The pronounced sensory and textural diversity observed across *M. longifolia* accessions highlights the underlying texture and sensory complexity of the different accessions. Variations in firmness, elasticity, and chewiness resemble patterns previously documented in grape, berries datesand apple [9–13], indicating that mechanical properties of floral tissues are strongly genotype-dependent and likely governed by differential cell-wall organization and moisture retention capacity. Such diversity underscores the importance of identifying accessions aligned with consumer-preferred softness and sweetness for optimized processing applications.

 doi:10.20944/preprints202602.1486.v1

3.2. The Biochemical Analysis of Primary Metabolites in Developmental Stages of Flowering in Contracting Accession of M. longifolia

The biochemical analysis of *M. longifolia* flowers across accessions (BM-1, BM-4, BM-5, BM-6, BM-10) showed significant developmental variation. BM-5 had the highest total sugar in mature flowers, indicating greater sweetness, consistent with earlier findings [14,15]. Reducing sugars were higher in immature flowers, indicating intense metabolic activity during early development, whereas non-reducing sugars increased at maturity, reflecting conversion and accumulation of sucrose for reproductive and storage functions. Developmental regulation of sugar metabolism and interconversion between sugar forms has been widely reported in plants [16], and Mahua flowers exhibit dynamic carbohydrate changes during maturation [17], with sugars also contributing to floral metabolite biosynthesis [16–18]. BM-5 total sugar was comparable to ripened grapes [19,20], supporting its superior palatability.Protein content peaked in immature BM-1 and mature BM-5 flowers, aligning with reported ~6.37% protein in *M. longifolia* [21,22]. β-carotene was highest in immature BM-5 and decreased with maturity, similar to observations in vegetable [23]. Lycopene levels were high in immature BM-5 and mature BM-4, comparable to values in beetroot and tomato [24,25], highlighting *M. longifolia*'s functional food potential.

Betanin was present in both immature and mature flowers of BM-4 and BM-5, similar to levels in pitaya and garambullo [26,27], supporting its use as a natural colorant. A stage-dependent shift in pigments, also seen in *Tageteserecta* [28], suggests a common developmental trend across species. Vitamin C content varied by tissue and stage, with maximum levels in BM-4, &BM-5 mature flowerand immature flower of BM-10 matching earlier reports [16,29]. DPPH-based antioxidant activity was highest among immature flowers, with BM-1 showing comparatively higher antioxidant capacity, whereas BM-5 exhibited the highest antioxidant activity among mature flowers. The antioxidant levels in immature BM-1 and mature BM-5 flowers were comparable to those reported for red grapes and grape pulp.[30,31], indicating strong health-promoting potential. Crude fiber and Phenol were highest in all immature flower stages aligning with previously reported values [14,32,35]. Although phenolics and β-carotene were higher in immature flowers, the increased antioxidant activity observed in mature flowers may be attributed to the cumulative and synergistic effects of multiple bioactive compounds, including lycopene, betanin, sugars, and other secondary metabolites that increase during maturation. Additionally, changes in the chemical structure, extractability, and bioavailability of antioxidant compounds during flower development may enhance radical scavenging capacity in mature flowers. The contribution of non-phenolic antioxidants and Maillard reaction products formed during maturation may also play a role in increasing antioxidant activity [34,35]. Furthermore, the antioxidant assays such as DPPH measure the overall radical scavenging capacity, which reflects the combined effect of all antioxidants rather than individual compounds.

Thus, both accession and developmental stage significantly shape the nutritional and phytochemical profile of *M. longifolia*. Accessions such as BM-5 and BM-4, with superior sweetness, pigments, antioxidants, and nutrients, show strong potential for value-added products, natural supplements, and functional food applications.

3.3. Elemental Composition of M. longifolia Flower in Contrasting Accessions by ICP–MS

Mineral diversity revealed by ICP–MS emphasizes the nutritional importance of *M. longifolia*, as many accessions contained higher elemental levels than Brassica or nasturtium flowers [36,37]. Sensory modulation by minerals is well-established: Na enhances sweetness and suppresses bitterness via ENaC-mediated pathways [39], while Ca and Mg influence taste through TRPM5 and TRPV1 activation [40,41] and contribute to kokumi perception [41]. The presence of Fe- and Zn-associated metallic notes [42,43] may further shape accession-specific palatability. These mineral–taste interactions demonstrate that the flavor quality of *M. longifolia* flowers is not solely sugar-driven but is also influenced by ionic balance [43,44]. Their high essential mineral content additionally reinforces the species value as a functional food resource.

 doi:10.20944/preprints202602.1486.v1

3.4. GC–MS-Based Secondary Metabolite Profiling and KEGG Pathway Mapping in Developing Flowers of Contrasting M. longifolia Accessions (BM1&BM5)

GC–MS profiling of *M. longifolia* accessions BM-1 and BM-5 across immature and mature stages revealed developmental and accession-specific differences, with BM-5—particularly at maturity—showing the highest VOC diversity and the greatest number of unique metabolites. BM-1 displayed a more conserved profile, while both accessions shared a core set of compounds. Immature flowers were richer in alcohols and ethers, whereas mature flowers contained more small sugar, ketones and esters, with terpenes present throughout, consistent with the sesquiterpene and (E,E)-farnesol dominance previously reported in *M. longifolia* [18]. Similar ranges of VOC richness have been observed in other flowers, including roses [45], *Luculiapinceana* [46], *Tillandsia* species [47,48], and *Lycoris taxa* [49], as well as in other metabolite-rich plants such as *Asparagus* bean seeds [50].

Integrated VOC and KEGG pathway analyses further revealed clear metabolic reprogramming during floral development. Immature flowers showed enrichment in alkaloid, terpenoid, phenylpropanoid, and carbon metabolism pathways, while mature flowers shifted toward hormone, terpenoid, and steroid biosynthesis. These developmental trends reflect the functional roles of floral VOCs in defense and pollinator signaling [51–53], and align with established MEP/MVA pathway contributions to terpenoid and phenylpropanoid formation [54–56]. Sulfur- and nitrogen-containing volatiles also support ecological communication [49]. Overall, BM-5 exhibits greater metabolic plasticity and VOC diversification, highlighting its strong potential for aromatic, industrial, ecological, and therapeutic applications.

3.5. Integrated Hierarchical Clustering, VIP Score, and Volcano Plot Analyses, Reveals Developmental Regulation of Key Metabolites in Contrasting M. longifolia Accessions

The integrated metabolomic profiling of *M. longifolia* flowers clearly demonstrates that floral development drives a strong and structured biochemical shift, separating immature and mature stages across clustering, VIP, and volcano analyses. This developmental transition aligns with pathways that enhance aroma formation, nutritional stability, and processing suitability—traits vital for fermentation industries, flavor extraction, nutraceutical applications, and broader bio-based utilization. A key outcome of maturation is the marked accumulation of furan derivatives such as furfural, 5-HMF, and Methylfurfural, most prominently in BM-5. These Maillard-derived compounds confer roasted, caramel-like, and sweet aromatic notes, making mature flowers naturally richer in flavor precursors [57–59]. Their elevated presence in BM-5 indicates strong suitability for high-aroma distillates and enhanced fermentation complexity [60,61]. Beyond sensory functions, compounds such as 5-HMF exhibit antioxidant, anti-allergic, anti-inflammatory, anti-hypoxic, anti-sickling, and anti-hyperuricemic effects and functional bioactive properties, supporting their relevance in natural preservatives and plant-based flavor enhancers [62–64]. The strong anti-inflammatory effects of 5 HMF in LPS-activated macrophages by suppressing MAPK, NF-κB, andAkt/mTOR signaling pathways. It shows promise as a bioactive functional-food ingredientwith therapeutic potential [65].

Immature flowers, in contrast, show higher levels of fatty-acid derivatives and long-chain aldehydes—particularly in BM-5—indicating early activation of lipid metabolism essential for membrane stability and developmental readiness. Fatty acid esters like methyl stearate and linoleic acid methyl ester have industrial significance as precursors for bio-lubricants, emulsifiers, and surfactants, widening *M. longifolia*'s potential into pharmaceutical applications [66,67]. Such stage specificity highlights the importance of selective harvesting for maximizing targeted metabolite yields.

Terpenoid-associated metabolites (Lupeol acetate, Epilupeol, Supraene, β-Amyrin) dominate immature BM-5 flowers, reinforcing their pharma industrial value [68]. These compounds—known for anti-inflammatory, antimicrobial, wound-healing, and antioxidant properties—strongly support the use of immature flowers for nutraceutical and herbal formulations [69–72]. Their decline at maturity further underscores the critical timing required to capture peak bioactivity. Nitrogenous and phenolic volatiles, including benzyl nitrile and 4-hydroxybenzaldehyde, were also significantly

 doi:10.20944/preprints202602.1486.v1

elevated in BM-5, suggesting greater metabolic investment in aroma and stress-responsive compounds [73].

Distinct stage- and accession-linked differences were also evident in sugars, fatty acids, and related derivatives. Sugar-derived metabolites also show meaningful accession-specific patterns. Sugars such as β-D-Glucopyranose, D-Allose, and Melibiose displayed characteristic patterns linked to energy regulation and osmotic balance [74,75]. Levoglucosan and Melibiose indicate differential carbohydrate mobilization and stress response, while the detection of D-Allose in BM-1 mature flowers is noteworthy due to its reported insulin-sensitizing, anti-inflammatory, and cytoprotective activities [75–78]. Quinic acid, consistently detected across stages, contributes as a precursor to chlorogenic acids and enhances the nutritional value of *M. longifolia*-based foods and beverages [79].

Flavonoid glycosides like flavone 4′-OH,5-OH,7-di-O-glucoside were enriched in immature BM-1 flowers, indicating roles in defense, pigmentation, and antioxidant activity [80]. Fatty acids, including Palmitic acid and Polyunsaturated species, showed dynamic modulation supporting membrane stability and signaling [81,82], while methyl isostearate in BM-5 immature flowers suggests active ester biosynthesis pathways [83].

Furan and pyran derivatives—furfural, HMF, Furaneol, Maltol, Allomaltol, and 4H-Pyran-4-one compounds—were especially abundant in BM5MF, reflecting intensified sugar degradation and Maillard reaction activity [84–87]. Mechanistically, MF conditions favor furan and furanone formation through sugar–amino acid interactions, whereas IMF stages suppress these reactions due to lower moisture or altered pH. BM-5 MF showed the strongest Maillard signature, suggesting superior potential for aroma enhancement [88], while BM-1 MF maintained higher native sugars and flavonoids, balancing primary and secondary metabolism.

Overall, IMF stages favored bioactive secondary metabolites (flavonoids, cyclitols, polyunsaturated fatty acids), whereas MF stages enhanced sugars, triterpenoids, and Maillard products. BM-5 consistently displayed stronger accumulation of furans and triterpenoids, reflecting higher metabolic capacity. The interplay of developmental stage, accession genetics, and biochemical reprogramming clearly shapes *M. longifolia*'s aroma, nutritional, and industrial potential.

From a processing viewpoint, these findings provide a practical blueprint for value-addition. Immature flowers are optimal for triterpenoid-rich nutraceuticals, while mature flowers offer superior substrates for flavor extraction, fermentation-based beverages, and aroma standardization. Accession-specific metabolic fingerprints enable targeted extraction strategies for furans, esters, and terpenoids and facilitate the development of standardized, quality-controlled *M. longifolia*-based flavor and nutraceutical products. Together, these insights support the design of accession-specific valorization pipelines that align metabolite strengths with industrial applications and market-driven product innovation.

4. Materials and Methods

4.1. Collection of Immature and Mature Flower of M. longifolia

M. longifolia orchards located within the Banda University of Agriculture and Technology (BUAT), Banda campus, Uttar Pradesh, were selected for the present study (Figure 1a). The taxonomic identity different *M. longifolia*accessions was confirmed and authenticated by the National Botanical Research Institute (NBRI), Lucknow (Figure 1b). Immature and mature flowers were collected during the morning hours directly from the campus orchards. Freshly collected samples were then processed for further experimental analysis

 doi:10.20944/preprints202602.1486.v1

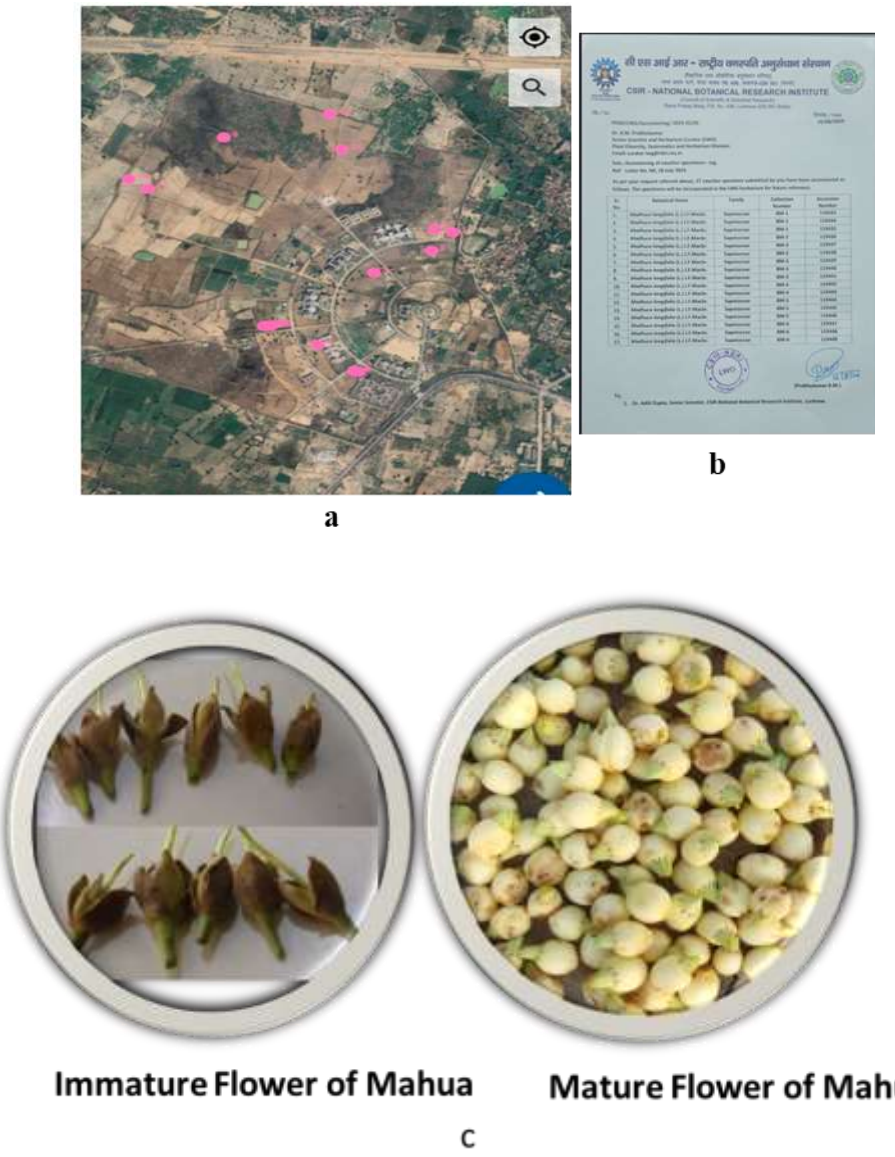

Figure 9. a) Location of the *M. longifolia* orchard at Banda University of Agriculture and Technology (BUAT), Banda, Uttar Pradesh, India. **b)** Their authenticity was confirmed by the National Botanical Research Institute (NBRI), Lucknow, and voucher specimens were deposited for future reference. **c)** immature and maturre flower of *M. longifolia.*

4.2. Sensory and Instrumental Texture Analysis

A sensory evaluation of different *M. longifolia*accessions BM-1-BM-13 flowers was performed using a 9-point hedonic scale by a panel of seven judges. Samples, coded with three-digit identifiers, were assessed for appearance, juiciness, texture, aroma, and sweetness. Each judge evaluated ten anonymous samples, expressing preferences from “Dislike Extremely” (1) to “Like Extremely” (9) [89]. Texture measurements of *M. longifolia* flowers from 13 accessions were conducted using a TA.XT Express Connect Texture Analyzer (Stable Micro Systems Ltd., UK) with a 10 kg load cell and Express Connect Lite software. Tests in compression and tension were performed at a speed range of 0.1–10 mm/s, with a maximum testing pressure of 210 mm. Five berries from each accessions were tested at room temperature (25 °C) using a P/2 probe (2 mm cylinder). Test parameters included pre-test speed (1.50 mm/s), test speed (1.00 mm/s), post-test speed (10.00 mm/s), distance (6.00 mm), strain (10%), and trigger force (5 g). Skin strength and elasticity were derived from the force–time curve.

 doi:10.20944/preprints202602.1486.v1

4.3. Biochemical Analysis of Primary Metabolites

M. longifolia flowers from selected accessions were analyzed at immature and mature stages for primary metabolites.

4.3.1. Carbohydrates

Total carbohydrates were estimated using phenol–sulfuric acid, with absorbance at 490 nm. Reducing sugars were determined by method using alkaline copper tartrate and arsenomolybdate reagents, with absorbance at 510 nm [91–93]. Non-reducing sugars were calculated as the difference between total and reducing sugars.

4.3.2. Protein

Protein was extracted in Tris-HCl buffer (pH 7.5) and estimated by method using Folin's phenol reagent, with BSA as the standard [94].

4.3.3. Ascorbic Acid

Quantified by titration with 2,6-dichlorophenol indophenol using oxalic acid extracts [95].

4.3.4. Antioxidant Activity

Measured by the DPPH radical scavenging assay [96], with absorbance recorded at 517 nm after incubation in the dark.

4.3.5. β-Carotene

Extracted with acetone–petroleum ether and quantified spectrophotometrically at 452 nm [97].

4.3.6. Total Phenolic Content

Estimated using Folin–Ciocalteu reagent in alkaline medium with catechol as the standard [98].

4.4. Mineral Analysis by ICP-MS

Mineral content in *M.longifolia* flowers was quantified using Inductively Coupled Plasma Mass Spectrometry (ICP-MS; Model: Agilent ICP-MS 7850),. Flower samples from each stage and accession were washed, oven-dried at 60 °C, and ground into a fine powder. 0.5 g of the sample was digested with concentrated nitric acid (HNO_3) and hydrogen peroxide (H_2O_2) using a microwave digestion system (Model: Microwave Digestion System, Multiway GO Plus (Anton Paar), followed by dilution with deionized water. Digested samples were analyzed using ICP-MS, with calibration performed using certified multi-element standards and internal standards to correct for instrumental drift. Each sample was analyzed in triplicate, and mineral concentrations were expressed as mg/kg dry weight. Blanks and standard reference materials were included to ensure accuracy and reproducibility. Statistical analysis was performed to compare mineral profiles in different accessions [99]

4.5. GC-MS Analysis

4.5. 1Extraction of Volatile Compounds

Each sample were accurately weighed 5 g ± 0.0005, transferred to 50 mL centrifuge tube, add 25 ml Methanol: n-Hexane (99: 1%v/v) then Vortex each at same moment for 60 min using *NeuationiSwix* MV Multi Vortex Mixer at 2500 rpm, centrifuge at 10,000 rpm at 10 °C for 10 min. Then transfer 5ml of supernatant in 20 ml glass tube and evaporate the solution completely at 40 °C and then reconstitute it up to 2 ml in methanol which subjected to filter through 0.45 um PVDF filter and used for analysis purposes.

 doi:10.20944/preprints202602.1486.v1

4.5.2. GC-MS Analysis and Data Interpretation

The GC-MS analysis was performed on an Agilent 8890 gas chromatograph coupled with an Agilent 5977B MS detector (GC-MS) (Agilent, Santa Clara, CA, USA). The separation of volatile compounds was carried out on a DB-5MS capillary column (30 m × 0.32 mm × 0.25 μm film thickness). Helium (purity > 99.999%) was employed as carrier gas with a constant flow rate of 1.2 mL/min. The injection volume was 1 μL. Temperature of injection port was set at 250 °C. The pulsed splitless mode was used. The oven temperature was set at 45 °C at the initial stage for 3 min then increased to the to 200 °C at 5 °C/min hold for 10 min followed by final temperature of 250 °C at the rate of 40 °C/min and held for 20 min. The mass spectrometry was conducted with ionization mode of EI with electron energy of 70 eV. The temperature of ion source and quadrupole were set at 280 °C and 150 °C, respectively. Full scan mode was applied with a mass scan range of 35–800 atomic mass unit (amu). Data processing for compounds identification was performed by using Wiley Registry 12th Edition / NIST 2020 Mass Spectral Library by MassHunter Workstation Qualitative Analysis Version 10.0.10305.0 (Agilent Technologies, Palo Alto, CA, USA).

Volatile compounds were identified by comparing retention indices (RI), calculated using a C7–C30 n-alkanes standard mixture, and mass spectral fragmentation patterns with corresponding Kovats indices and mass spectra from the Wiley Registry 12th Edition/NIST 2020 library, using MassHunter Workstation Qualitative Analysis software, as well as with published literature data [103,104].

4.6. Statistical, KEGG, Variable Importance in Projection (VIP) and Data Analysis

The study was conducted using a Completely Randomized Design. Statistical analyses, including ANOVA, were performed using OPSTAT (CCSHAU, Hisar) and SPSS software. GC–MS data were processed to identify and quantify metabolites using software Agilent MassHunter. The resulting peak area matrix was normalized and scaled, followed by Partial least squares discriminant analysis (PLS-DA to assess group separation. Variable Importance in Projection (VIP) scores were then calculated from the PLS model based on variable weights and explained variance, with compounds showing VIP values greater than 1 considered significant contributors to sample differentiation [102]. Differentially expressed metabolites were mapped to the KEGG database for pathway enrichment analysis. KEGG enrichment was performed with a significance threshold of FDR $q \leq 0.05$ [105,106].

5. Conclusions

This work provides the first integrated, multi-trait characterization of *M. longifolia* flower accessions by combining texture profiling, nutritional and phytochemical analysis, mineral composition, and comprehensive GC–MS–based metabolomics across developmental stages. Such a holistic dataset has not been reported previously for *M. longifolia*. Early-stage flowers were dominated by fatty-acid esters, aldehydes, flavonoid glycosides, and terpenoids, while mature flowers transitioned toward carbohydrate-derived volatiles, particularly furans, pyranones, esters, and other aroma-active compounds. Among all accessions, BM-5 displayed the most diverse and responsive metabolic profile, characterized by higher sugars, carotenoids, and a broader array of volatiles, including key fermentation and aroma markers such as melibiose and furfural, 5-HMF, and furaneol respectively. Its enrichment in several biologically relevant metabolites further strengthens its suitability for food, aromatic, and health-oriented applications. Multivariate and pathway analyses consistently supported BM-5 as the most metabolically flexible accession.

Overall, this integrated analysis establishes clear accession-specific strengths that can guide targeted utilization. BM-5 is best aligned with flavor, fermentation, distillation, and nutraceutical industries, while BM-1 and BM-4 provide valuable profiles for antioxidant- and protein-rich formulations. These insights address the current lack of accession-specific guidelines for *M. longifolia*

 doi:10.20944/preprints202602.1486.v1

valorization and create new opportunities for cultivar selection, processing optimization, and sustainable commercialization of this culturally and economically important tree species.

Supplementary Materials: The following supporting information can be downloaded at the website of this paper posted on Preprints.org, Supplementary Table S1: Texture analysis and Sensory evaluation of *M. longifolia* Flower collected from different accession from BUAT Campus. Supplementary Table S2a List of secondary metabolites compound identified by GS-MS in Immature Flower of *M.longifolia* accession BM-1. Supplementary Table S2b: List of secondary metabolites compound identified by GS-MS in mature Flower of *M.longifolia* accession BM-1. Supplementary Table S3a:List of secondary metabolites compound identified by GS-MS in Immature Flower of *M.longifolia* accession BM-5. Supplementary Table S3b:List of secondary metabolites compound identified by GS-MS in mature Flower of *M.longifolia* accession BM-5. Supplementary table S4: VIP Score of secondary metabolites compound identified by GS-MS in contrasting accession and developmental stages of *M.longifolia.* Supplementary Table S5. Differential metabolites identified by volcano plot analysis comparing immature and mature flower stages between contrasting *M.longifolia* accessions (BM1 and BM5).

Author Contributions: SP, AR conceived the idea and planned the work,; RPJ, and AV performed the experiment; AR,VM, did analysis of texture property; RPJ, AA did GCMS; NK did ICPMS; AV ,SP write the manuscript; VC, CMS, AS and AK edited the manuscript and. All authors read the manuscript and approved it for publication.

Funding: This research did not receive any, specific grant from funding agencies in the public, commercial, or not-for-profit sectors.

Institutional Review Board Statement: Not applicable.

Informed Consent Statement: Not applicable.

Data Availability Statement: All data generated or analyzed during this study are included in this published article (and its Supplementary Materials).

Acknowledgments: The authors extend their appreciation to the Researchers Supporting Project No. (BUAT/DR/2020/282/9) at Banda, University of Agriculture and Technology, Banda.

Conflicts of Interest: The authors declare no conflicts of interest.

Abbreviation

KEGG	***Kyoto Encyclopedia of Genes and Genomes***
GC–MS	***Gas Chromatography–Mass Spectrometry***
PCA	***Principal Component Analysis***
VIP	**Variable Importance in Projection**

References

1. Gupta, A.; Sanwal, N.; Sharma, N.; Sahu, J.K.; P, H.; Kheto, A. Dynamics of functional and physicochemical properties of *Madhuca longifolia* flower juice under *Saccharomyces cerevisiae* fermentation. Food and Humanity2024, *2*, 100244. https://doi.org/10.1016/j.foohum.2024.100244
2. Mishra, A.; Poonia, A. *mahua* (*Madhuca longifolia*) flowers: Review on processing and biological properties. Nutr. Food Sci.2019, *49*, 1153–1163.
3. Gupta, A.; Chaudhary, R.; Sharma, S. Potential applications of *mahua* (*Madhuca indica*) biomass. Waste Biomass Valorization2012, *3*, 175–189.
4. Singh, D.; Yadav, E.; Kumar, V.; Verma, A. *Madhuca longifolia*-embedded silver nanoparticles attenuate diethylnitrosamine (DEN)-induced renal cancer via regulating oxidative stress. Curr. Drug Deliv.2021, *18*, 634–644.
5. Baschali, A.; Tsakalidou, E.; Kyriacou, A.; Karavasiloglou, N.; Matalas, A.L. Traditional low-alcoholic and non-alcoholic fermented beverages consumed in European countries: A neglected food group. Nutr. Res. Rev.2017, *30*, 1–24.

 doi:10.20944/preprints202602.1486.v1

6. Jayabalan, R.; Waisundara, V.Y. Kombucha as a functional beverage. In Functional and Medicinal Beverages; Academic Press: London, UK, 2019; pp. 413–446.
7. Singh, V.; Kumar, S.; Rai, A.K. Sensory analysis of bar samples prepared from *mahua* (*Madhuca longifolia*) flower syrup using fuzzy logic. Nutrafoods2018, *17*, 137–144.
8. Pooja; Purohit, A.; Kaur, S.; Yadav, S.K. Identification of a yeast *Meyerozymacaribbica* M72 from mahua flower for efficient transformation of rice straw into ethanol. *Biomass Convers. Biorefin.* 2023, *13*, 12591–12603.
9. Cejudo-Bastante, M.J.; Rodríguez-Pulido, F.J.; Heredia, F.J.; González-Miret, M.L. Assessment of sensory and texture profiles of grape seeds at real maturity stages using image analysis. Foods2021, *10*, 1098. https://doi.org/10.3390/foods10051098
10. Liu, M.; Liu, M.; Bai, L.; Shang, W.; Ren, R.; Zhao, Z.; Sun, Y. Establishing a berry sensory evaluation model based on machine learning. Foods2023, *12*, 3502. https://doi.org/10.3390/foods12183502
11. Quispe-Sanchez, L.; Mena-Chacon, L.M.; Hernandez-Diaz, E.; Siche, R.; Yoplac, I.; Chuquilín-Goicochea, R.; Vigo, C.N.; Juarez-Contreras, L.; Oliva-Cruz, M. Physicochemical, functional, and sensory properties of berries at different maturity stages. Appl. Food Res.2025, *5*, 101265. https://doi.org/10.1016/j.afres.2025.101265
12. Singh, V.; Guizani, N.; Al-Zakwani, I.; Al-Shamsi, Q.; Al-Alawi, A.; Rahman, M.S. Sensory texture of date fruits as a function of physicochemical properties and its use in date classification. Acta Aliment.2015, *44*, 119–125.
13. Gatti, E.; Di Virgilio, N.; Magli, M.; Predieri, S. Integrating sensory analysis and hedonic evaluation for apple quality assessment. J. Food Qual.2011, *34*, 126–132.
14. Swain, M.R.; Kar, S.; Sahoo, A.K.; Ray, R.C. Ethanol fermentation of mahula (*Madhuca latifolia* L.) flowers using free and immobilized yeast *Saccharomyces cerevisiae*. Microbiol. Res.2007, *162*, 93–98.
15. Pandey, A.K.; Rakesh, S. *Madhuca longifolia* var. *latifolia* (Roxb.) A. Chev: A plant with medicinal boon. Int. J. Ayurvedic Med.2023, *14*, 593–605.
16. Li, M.; Li, P.; Ma, F.; Dandekar, A.M.; Cheng, L. Sugar metabolism and accumulation in the fruit of transgenic apple trees with decreased sorbitol synthesis. Hortic. Res.2018, *5*, 60. https://doi.org/10.1038/s41438-018-0064-8
17. Lungade, P.; Karadbhajne, S.V. Mahua flower (*Madhuca indica*): Approach of functional, nutritional characteristics and an accompaniment to food products. J. Pharm. Negat. Results2022, *13*, 9093–9104.
18. Suryawanshi, Y.C.; Mokat, D.N. Chemical composition of essential oil of *Madhuca longifolia* var. *latifolia* (Roxb.) A. Chev. flowers. J. Essent. Oil Bear. Plants2019, *22*, 1034–1039.
19. Ferrara, G.; Marcotuli, V.; Didonna, A.; Stellacci, A.M.; Palasciano, M.; Mazzeo, A. Ripeness prediction in table grape cultivars by using a portable NIR device. Horticulturae2022, *8*, 613.
20. Herrera, J.; Guesalaga, A.; Agosin, E. Shortwave–near infrared spectroscopy for non-destructive determination of maturity of wine grapes. Meas. Sci. Technol.2003, *14*, 689–697.
21. Kureel, R.S.; Kishor, R.; Dutt, D.; Pandey, A. Mahua : A Potential Tree Borne Oilseed; National Oilseeds and Vegetable Oils Development Board, Ministry of Agriculture, Government of India: Gurugram, India, 2009; pp. 1–21.
22. Sinha, J.; Singh, V.; Singh, J.; Rai, A.K. Phytochemistry, ethnomedical uses and future prospects of Mahua (*Madhuca longifolia*) as a food: A review. J. Nutr. Food Sci.2017, *7*, 573.
23. Kassaye, M.; Hagos, M.; Chandravanshi, B.S. Determination of β-carotene in five commonly used Ethiopian vegetables using UV–Vis spectrophotometric method. Chem. Int.2023, *9*, 111–119.
24. Sultana, R.; Polash, M.A.S.; Sakil, M.A.; Shorna, S.I.; Rahman, M.S.; Rahman, M.A.; Hossain, M.A. Health-promoting pigments and bioactive compounds of six vegetables grown in Bangladesh. Asian J. Med. Biol. Res.2019, *5*, 280–285.
25. Suwanaruang, T. Analyzing lycopene content in fruits. Agric. Agric. Sci. Procedia2016, *11*, 46–48.
26. Sandate-Flores, L.; Rodríguez-Hernández, D.V.; Rostro-Alanis, M.; Melchor-Martínez, E.M.; Brambila-Paz, C.; Sosa-Hernández, J.E.; Iqbal, H.M.N. Evaluation of three methods for betanin quantification in fruits from cacti. MethodsX2022, *9*, 101746.

 doi:10.20944/preprints202602.1486.v1

27. Choo, K.Y.; Ong, Y.Y.; Lim, R.L.H.; Tan, C.P.; Ho, C.W. Study on bioaccessibility of betacyanins from red dragon fruit (*Hylocereuspolyrhizus*). Food Sci. Biotechnol.2019, *28*, 1163–1169.
28. Qiu, Y.; Wang, R.; Zhang, E.; Shang, Y.; Feng, G.; Wang, W.; Ma, Y.; Bai, W.; Zhang, W.; Xu, Z.; Shi, W.; Niu, X. Carotenoid biosynthesis profiling unveils the variance of flower coloration in *Tageteserecta* and enhances fruit pigmentation in tomato. Plant Sci.2024, *347*, 112207. https://doi.org/10.1016/j.plantsci.2024.112207
29. Jayasree, B.; Harishankar, N.; Rukmini, C. Chemical composition and biological evaluation of *Mahua* flowers. Indian J. Nutr. Diet.1998, *35*, 1–6.
30. Muzolf-Panek, M.; Waśkiewicz, A. Relationship between phenolic compounds, antioxidant activity and color parameters of red table grape skins using linear ordering analysis. Appl. Sci.2022, *12*, 6146.
31. Nile, S.H.; Kim, S.H.; Ko, E.Y.; Park, S.W. Polyphenolic contents and antioxidant properties of different grape (*Vitisvinifera*, *V. labrusca*, and *V. hybrid*) cultivars. Biomed Res. Int.2013, *2013*, 718065.
32. Dwivedi, A.; Priyadarshini, A.; Induar, S. Mahua (*Madhuca longifolia*) flower and its application in food industry: A review. Int. J. Chem. Stud.2022, *10*, 80–84.
33. Zheng, J.; Yu, X.; Maninder, M.; Xu, B. Total phenolics and antioxidants profiles of commonly consumed edible flowers in China. Int. J. Food Prop.2018, *21*, 1524–1540.
34. Zhang, C.;Guo, X.;Guo, R.; Zhu, L.;Qiu, X.; Yu, X.; Chai, J.;Gu, C.;&Feng, Z. (2023). Insights into the effects of extractable phenolic compounds and Maillard reaction products on the antioxidant activity of roasted wheat flours with different maturities. Food Chemistry: 2023, 17, 100548. https://doi.org/10.1016/j.fochx.2022.100548
35. Bolchini, S.; Morozova, K.; Ferrentino, G.; Scampicchio, M. Assessing antioxidant properties of Maillard reaction products: Methods and potential applications as food preservatives. *Eur. Food Res. Technol.*2025, *251*, 2039–2059. https://doi.org/10.1007/s00217-025-04770-6
36. Sood, S.; Methven, L.; Cheng, Q. Role of taste receptors in salty taste perception of minerals and amino acids and developments in salt reduction strategies: A review. *Crit. Rev. Food Sci. Nutr.* 2025, *65*, 3444–3458.
37. Jakubczyk, K.; Janda, K.; Watychowicz, K.; Łukasiak, J.; Wolska, J. Garden nasturtium (*Tropaeolummajus* L.)—A source of mineral elements and bioactive compounds. Rocz. Panstw. Zakl. Hig.2018, *69*, 119–126.
38. Sood, S.; Methven, L.; Cheng, Q. Role of taste receptors in salty taste perception of minerals and amino acids and developments in salt reduction strategies: A review. *Crit. Rev. Food Sci. Nutr.* 2025, *65*, 3444–3458.
39. Ahern, G.P.; Brooks, I.M.; Miyares, R.L.; Wang, X.-B. Extracellular cations sensitize and gate capsaicin receptor TRPV1 modulating pain signaling. J. Neurosci.2005, *25*, 5109–5116.
40. Riera, C.E.; Vogel, H.; Simon, S.A.; Damak, S.; le Coutre, J. Sensory attributes of complex tasting divalent salts are mediated by TRPM5 and TRPV1 channels. J. Neurosci.2009, *29*, 2654–2662.
41. Medler, K.F. Calcium signaling in taste cells. Biochim. Biophys. Acta Mol. Cell Res.2015, *1853*, 2025–2032.
42. Keast, R.S. The effect of zinc on human taste perception. J. Food Sci.2003, *68*, 1871–1877.
43. Orth, H.N.; Pirkwieser, P.; Benthin, J.; Koehler, M.; Sterneder, S.; Parlar, E.; Schaudy, E.; Lietard, J.; Michel, T.; Boger, V.; Dunkel, A.; Somoza, M.M.; Somoza, V. Bitter taste receptor TAS2R43 co-regulates mechanisms of gastric acid secretion and zinc homeostasis. Int. J. Mol. Sci.2024, *26*, 6017. https://doi.org/10.3390/ijms26136017
44. Huseynli, L.; Walser, C.; Blumenthaler, L.; Vene, K.; Dawid, C. Toward a comprehensive understanding of flavor of sunflower products: A review of confirmed and prospective aroma- and taste-active compounds. Foods2025, *14*, 1940.
45. Quan, W.; Jin, J.; Qian, C.; Li, C.; Zhou, H. Characterization of volatiles in flowers from four *Rosa chinensis* cultivars by HS-SPME-GC×GC-QTOFMS. Front. Plant Sci.2023, *14*, 1060747.
46. Li, S.; Dong, M.; Yang, J.; Cheng, X.; Shen, X.; Liu, S.; Han, B. Selective hydrogenation of 5-(hydroxymethyl)furfural to 5-methylfurfural over single atomic metals anchored on Nb_2O_5. Nat. Commun.2021, *12*, 584.
47. Gonzalez, A.; Benfodda, Z.; Bénimélis, D.; Fontaine, J.X.; Molinié, R.; Meffre, P. Extraction and identification of volatile organic compounds in scentless flowers of 14 *Tillandsia* species using HS-SPME/GC-MS. Metabolites2022, *12*, 628.

 doi:10.20944/preprints202602.1486.v1

48. Lo, M.M.; Benfodda, Z.; Bénimélis, D.; Fontaine, J.X.; Molinié, R.; Meffre, P. Extraction and identification of volatile organic compounds emitted by fragrant flowers of three *Tillandsia* species by HS-SPME/GC-MS. Metabolites2021, *11*, 594.
49. Shi, T.; Yue, Y.; Shi, M.; Chen, M.; Yang, X.; Wang, L. Exploration of floral volatile organic compounds in six typical *Lycoris* taxa by GC–MS. Plants2019, *8*, 422.
50. Perchuk, I.; Shelenga, T.; Gurkina, M.; Miroshnichenko, E.; Burlyaeva, M. Composition of primary and secondary metabolite compounds in seeds and pods of asparagus bean (*Vignaunguiculata* (L.) Walp.) from China. Molecules2020, *25*, 3778.
51. Darwish, A.G.; Das, P.R.; Olaoye, E.; Gajjar, P.; Ismail, A.; Mohamed, A.G.; Tsolova, V.; Hassan, N.A.; El Kayal, W.; Walters, K.J. Untargeted flower volatilome profiling highlights differential pollinator attraction strategies in muscadine. Front. Plant Sci.2025, *16*, 1548564. https://doi.org/10.3389/fpls.2025.1548564
52. Chautá, A.; Kumar, A.; Mejia, J.; Stashenko, E.E.; Kessler, A. Defensive functions and potential ecological conflicts of floral stickiness. Sci. Rep.2022, *12*, 19848. https://doi.org/10.1038/s41598-022-23261-2
53. Sasidharan, R.; Junker, R.R.; Eilers, E.J.; Müller, C. Floral volatiles evoke partially similar responses in both florivores and pollinators and are correlated with non-volatile reward chemicals. Ann. Bot.2023, *132*, 1–14. https://doi.org/10.1093/aob/mcad064
54. Basallo, O.; Perez, L.; Lucido, A.; Sorribas, A.; Vilaprinyo, E.; Albacete, A.; Fraser, P.D.; Christou, P.; Capell, T.; Alves, R. Changing biosynthesis of terpenoid precursors in rice through synthetic biology. Front. Plant Sci.2023, *14*, 1133299. https://doi.org/10.3389/fpls.2023.1133299
55. Dudareva, N.; Negre, F.; Nagegowda, D.A.; Orlova, I. Plant volatiles: Recent advances and future perspectives. Crit. Rev. Plant Sci.2006, *25*, 417–440.
56. Wang, Q.; Quan, S.; Xiao, H. Towards efficient terpenoid biosynthesis: Manipulating IPP and DMAPP supply. Bioresour. Bioprocess.2019, *6*, 1–13.
57. Liu, S.; Sun, H.; Ma, G.; Zhang, T.; Wang, L.; Pei, H.; Li, X.; Gao, L. Insights into flavor and key influencing factors of Maillard reaction products: A recent update. Front. Nutr.2022, *9*, 973677. https://doi.org/10.3389/fnut.2022.973677
58. Ho, C.T.; Zheng, X.; Li, S. Tea aroma formation. Food Sci. Hum. Wellness2015, *4*, 9–27.
59. Yang, W.; Zhang, C.; Li, C.; Huang, Z.Y.; Miao, X. Pathway of 5-hydroxymethyl-2-furaldehyde formation in honey. J. Food Sci. Technol.2019, *56*, 2417–2425.
60. Yang, J.; Jiang, D.; Shui, X.; Lei, T.; Zhang, H.; Zhang, Z.; Zhang, Q. Effect of 5-HMF and furfural additives on bio-hydrogen production by photo-fermentation from giant reed. Bioresour. Technol.2022, *347*, 126743.
61. Chen, C.; Lv, M.; Hu, H.; Huai, L.; Zhu, B.; Fan, S.; Zhang, J. 5-Hydroxymethylfurfural and its downstream chemicals: A review of catalytic routes. Adv. Mater.2024, *36*, 2311464.
62. Pagare, P.P.; McGinn, M.; Ghatge, M.S.; Shekhar, V.; Alhashimi, R.T.; Pierce, B.D.; Abdulmalik, O.; Zhang, Y.; Safo, M.K. The antisickling agent, 5-hydroxymethyl-2-furfural: Other potential pharmacological applications. Med. Res. Rev.2024, *44*, 2707–2729. https://doi.org/10.1002/med.22062
63. Fagbemi, K.O.; Aina, D.A.; Olutunmbi, M.; Naidoo, K.K.; Coopoosamy, R.M.; Olajuyigbe, O.O. Bioactive compounds, antibacterial and antioxidant activities of methanol extract of *Tamarindusindica* Linn. Sci. Rep.2022, *12*, 9432. https://doi.org/10.1038/s41598-022-13716-x
64. Shapla, U.M.; Solayman, M.; Alam, N.; Khalil, M.I.; Gan, S.H. 5-Hydroxymethylfurfural (HMF) levels in honey and other food products: Effects on bees and human health. Chem. Cent. J.2018, *12*, 35. https://doi.org/10.1186/s13065-018-0408-3
65. Kong, F.; Lee, B.H.; Wei, K. 5-Hydroxymethylfurfural mitigates lipopolysaccharide-stimulated inflammation via suppression of MAPK, NF-κB and mTOR activation in RAW 264.7 cells. Molecules2019, *24*, 275. https://doi.org/10.3390/molecules24020275
66. Sancheti, S.V.; Yadav, G.D. Synthesis of environment-friendly, sustainable, and nontoxic bio-lubricants: A critical review of advances and a path forward. Biofuels Bioprod. Biorefin.2022, *16*, 1172–1195.
67. Sharma, B.K.; Karmakar, G.; Shah, R.; Ghosh, P.; Sarker, M.I.; Erhan, S.Z. Sustainable lubricant formulations from natural oils: A short review. Renew. Sustain. Energy Rev.2023, *173*, 113095.

 doi:10.20944/preprints202602.1486.v1

68. Câmara, J.S.; Perestrelo, R.; Ferreira, R.; Berenguer, C.V.; Pereira, J.A.M.; Castilho, P.C. Plant-derived terpenoids: A plethora of bioactive compounds with several health functions and industrial applications—A comprehensive overview. Molecules2024, *29*, 3861. https://doi.org/10.3390/molecules29163861
69. Dalimunthe, A.; Gunawan, M.C.; Utari, Z.D.; Dinata, M.R.; Halim, P.; Pakpahan, N.E.S.; Sitohang, A.I.; Sukarno, M.A.; Harahap, Y.; Setyowati, E.P.; Park, M.N.; Yusoff, S.D.; Zainalabidin, S.; Prananda, A.T.; Mahadi, M.K.; Kim, B.; Harahap, U.; Syahputra, R.A. In-depth analysis of lupeol: Delving into the diverse pharmacological profile. Front. Pharmacol.2024, *15*, 1461478. https://doi.org/10.3389/fphar.2024.1461478
70. Sowa, R.M. The Pharmacological Potential of Lupeol and Derivatives: A Corroborative Analysis; Doctoral Dissertation, BRAC University: Dhaka, Bangladesh, 2022.
71. Liu, K.; Zhang, X.; Xie, L.; Deng, M.; Chen, H.; Song, J.; Luo, J. Lupeol and its derivatives as anticancer and anti-inflammatory agents: Molecular mechanisms and therapeutic efficacy. *Pharmacol. Res.* 2021, *164*, 105373.
72. Romero-Estrada, A.; Maldonado-Magaña, A.; González-Christen, J.; Bahena, S.M.; Garduño-Ramírez, M.L.; Rodríguez-López, V.; Alvarez, L. Anti-inflammatory and antioxidative effects of six pentacyclictriterpenes isolated from the Mexican copal resin of *Burseracopallifera*. BMC Complement. Altern. Med.2016, *16*, 422.
73. Liao, Y.; Zeng, L.; Tan, H.; Cheng, S.; Dong, F.; Yang, Z. Biochemical pathway of benzyl nitrile derived from L-phenylalanine in tea (*Camellia sinensis*) and its formation in response to post-harvest stresses. J. Agric. Food Chem.2020, *68*, 1397–1404.
74. Balabanlı, Z.Y. Investigating the Aqueous Behavior of D-Glucose, D-Fructose and D-Allulose by Molecular Dynamics Simulations and Nuclear Magnetic Resonance Relaxometry; Master's Thesis, Middle East Technical University: Ankara, Turkey, 2022.
75. Ma, X.L.; Wang, X.C.; Zhang, J.N.; Liu, J.N.; Ma, M.H.; Ma, F.L.; She, Y. A study of flavor variations during the flaxseed roasting procedure by developed real-time SPME GC–MS coupled with chemometrics. **Food Chem.2023**, *410*, 135453.
76. Van Laar, A.; Grootaert, C.; Rajkovic, A.; Desmet, T.; Beerens, K.; Van Camp, J. Rare sugar metabolism and impact on insulin sensitivity along the gut–liver–muscle axis in vitro. Nutrients 2023, 15, 1593.
77. Afzal, S.; Chaudhary, N.; Singh, N.K. Role of soluble sugars in metabolism and sensing under abiotic stress. In *Plant Growth Regulators: Signalling under Stress Conditions*; Springer: Cham, Switzerland, 2021; pp. 305–334.
78. Tan, M.J.; Ye, J.M.; Turner, N.; Hohnen-Behrens, C.; Ke, C.Q.; Tang, C.P.; Chen, T.; Weiss, H.C.; Gesing, E.R.; Ye, Y. Antidiabetic activities of triterpenoids isolated from bitter melon associated with activation of the AMPK pathway. Chem. Biol. 2008, 15, 263–273.
79. Clifford, M.N.; Kerimi, A.; Williamson, G. Bioavailability and metabolism of chlorogenic acids (acyl-quinic acids) in humans. Compr. Rev. Food Sci. Food Saf. 2020, 19, 1299–1352.
80. Agati, G.; Brunetti, C.; Di Ferdinando, M.; Ferrini, F.; Pollastri, S.; Tattini, M. Functional roles of flavonoids in photoprotection: New evidence, lessons from the past. Plant Physiol. Biochem. 2013, 72, 35–45.
81. Gomathi, D.; Kalaiselvi, M.; Ravikumar, G.; Devaki, K.; Uma, C. GC–MS analysis of bioactive compounds from the whole plant ethanolic extract of *Evolvulusalsinoides* (L.) L. J. *Food Sci. Technol.* 2015, 52, 1212–1217.
82. Yadav, S.; Suneja, P.; Hussain, Z.; Abraham, Z.; Mishra, S.K. Prospects and potential of Madhuca longifolia (Koenig) J.F. Macbride for nutritional and industrial purpose. Biomass Bioenergy 2011, 35, 1539–1544.
83. Saeed, N.M.; El-Demerdash, E.; Abdel-Rahman, H.M.; Algandaby, M.M.; Al-Abbasi, F.A.; Abdel-Naim, A.B. Anti-inflammatory activity of methyl palmitate and ethyl palmitate in different experimental rat models. Toxicol. Appl. Pharmacol. 2012, 264, 84–93.
84. Schwab, W. Natural 4-hydroxy-2,5-dimethyl-3(2H)-furanone (Furaneol®). Molecules 2013, 18, 6936–6951.
85. Yin, T.; Song, C.; Li, H.; Wang, S.; Wei, W.; Meng, J.; Liu, Q. Unveiling stage-specific flavonoid dynamics underlying drought tolerance in sweet potato (Ipomoea batatas L.) via integrative transcriptomic and metabolomic analyses. Plants 2025, 14, 2383.
86. Chan, P.N.A. Chemical properties and applications of food additives: Flavor, sweeteners, food colors, and texturizers. In Handbook of Food Chemistry; Springer: Berlin, Heidelberg, Germany, 2015; pp. 101–129.
87. Ahn, H.; Lee, G.; Han, B.C.; Lee, S.H.; Lee, G.S. Maltol, a natural flavor enhancer, inhibits NLRP3 and non-canonical inflammasome activation. Antioxidants 2022, 11, 1923.

 doi:10.20944/preprints202602.1486.v1

88. Cho, H.; Lee, K.G. Formation and reduction of furan in Maillard reaction model systems consisting of various sugars, amino acids, and furan precursors. J. Agric. Food Chem. 2014, 62, 5978–5982.
89. Gatti, E.; Di Virgilio, N.; Magli, M.; Predieri, S. Integrating sensory analysis and hedonic evaluation for apple quality assessment. J. Food Qual. 2011, 34, 126–132.
90. Manickavasagan, A.; Ganeshmoorthy, K.; Claereboudt, M.R.; Al-Yahyai, R.; Khriji, L. Non-destructive measurement of total soluble solid content of dates using near infrared imaging. Emir. J. Food Agric. 2014, 26, 970–978.
91. DuBois, M.; Gilles, K.A.; Hamilton, J.K.; Rebers, P.A.; Smith, F. Colorimetric method for determination of sugars and related substances. Anal. Chem. 1956, 28, 350–356.
92. Nelson, N. A photometric adaptation of the Somogyi method for the determination of glucose. J. Biol. Chem. 1952, 153, 375–380.
93. Somogyi, M. Notes on sugar determination. J. Biol. Chem. 1952, 195, 19–23.
94. Lowry, O.H.; Rosebrough, N.J.; Farr, A.L.; Randall, R.J. Protein measurement with the Folin phenol reagent. J. Biol. Chem. 1951, 193, 265–275.
95. Harris, L.J.; Ray, S.N. Determination of ascorbic acid in plant materials. Biochem. J. 1935, 29, 2013–2019.
96. Gupta, E.; Vajpayee, G.; Purwar, S.; Shakyawar, S.; Alok, S.; Sundaram, S. Phytochemical screening and in vitro studies of antioxidant and antimicrobial activity of extracts of dried Stevia rebaudiana leaves. Int. J. Pharm. Sci. Res. 2017, 8, 3354–3360. https://doi.org/10.13040/IJPSR.0975-8232.8(8).3354-60
97. Hagos, M.; Redi-Abshiro, M.; Chandravanshi, B.S.; Yaya, E.E. Development of analytical methods for determination of β-carotene in pumpkin (Cucurbita maxima) flesh, peel, and seed powder samples. Int. J. Anal. Chem. 2022, 2022, 9363692.
98. Kamtekar, S.; Keer, V.; Patil, V. Estimation of phenolic content, flavonoid content, antioxidant and α-amylase inhibitory activity of marketed polyherbal formulation. J. Appl. Pharm. Sci. 2014, 4, 061–065.
99. Ahmad, I.; Rawoof, A.; Dubey, M.; Ramchiary, N. ICP-MS based analysis of mineral elements composition during fruit development in Capsicum germplasm. J. Food Compos. Anal. 2021, 101, 103977.
100. Ma, C.; Li, J.; Chen, W.; Wang, W.; Qi, D.; Pang, S.; Miao, A. Study of aroma formation and transformation during the manufacturing process of oolong tea by SPME–GC–MS combined with chemometrics. Food Res. Int. 2018, 108, 413–422.
101. Shi, L.K.; Zhang, D.D.; Liu, Y.L. Survey of polycyclic aromatic hydrocarbons of vegetable oils and oilseeds by GC–MS in China. Food Addit. Contam. Part A 2016, 33, 603–611.
102. Wold, S.; Sjöström, M.; Eriksson, L. PLS-regression: A basic tool of chemometrics. Chemom. Intell. Lab. Syst. 2001, 58, 109–130.
103. Jaiswal, R.P.; Chugh, V.; Nagar, S.; Purwar, S.; Azam, A.; Verma, A. Screening of metabolites and metabolic pathways in five different Ocimum species from the same origin using GC–MS. Biochem. Res. Int. 2025, 2025, 7121687.
104. Lucero, M.; Estell, R.; Tellez, M.; Fredrickson, E. A retention index calculator simplifies identification of plant volatile organic compounds. Phytochem. Anal. 2009, 20, 378–384.
105. Kanehisa, M.; Araki, M.; Goto, S.; Hattori, M.; Hirakawa, M.; Itoh, M.; Katayama, T.; Kawashima, S.; Okuda, S.; Tokimatsu, T.; Yamanishi, Y. KEGG for linking genomes to life and the environment. Nucleic Acids Res. 2007, 36, D480–D484.
106. Xie, C.; Mao, X.; Huang, J.; Ding, Y.; Wu, J.; Dong, S.; Kong, L.; Gao, G.; Li, C.Y.; Wei, L. KOBAS 2.0: A web server for annotation and identification of enriched pathways and diseases. Nucleic Acids Res. 2011, 39, W316–W322